INEEL/EXT-01-01073

Test Results from SBW-FY01-PS-01 Vitrification Demonstration of Sodium Bearing Waste Simulant Using WM-180 Surrogate

K.J. Perry, R.R. Kimmitt, N.R. Soelberg, R.D. Tillotson, A.N. Olson

August 2001

Idaho National Engineering and Environmental Laboratory
Bechtel BWXT Idaho, LLC

INEEL/EXT-01-01073

Test Results from SBW-FY01-PS-01 Vitrification Demonstration of Sodium Bearing Waste Simulant Using WM-180 Surrogate

K.J. Perry, R.R. Kimmitt, N.R. Soelberg, R.D. Tillotson, A.N. Olson

August 2001

Idaho National Engineering and Environmental Laboratory

Idaho Falls, Idaho 83415

Prepared for the
U.S. Department of Energy
Office of Environmental Management
Under DOE Idaho Operations Office
Contract DE-AC07-99ID13727

ABSTRACT

Treatment of sodium-bearing waste (SBW) at the Idaho Nuclear Technology and Engineering Center (INTEC) within the Idaho National Engineering and Environmental Laboratory (INEEL) is mandated under a Settlement Agreement between the Department of Energy, the U.S. Navy, and the State of Idaho. One of the requirements of the Settlement Agreement is the complete calcination (i.e. treatment) of all SBW by December 31, 2012. One of the proposed options for treatment of SBW is vitrification.

This report describes the demonstration of the vitrification of WM-180 SBW surrogate waste using the SBW-9 formulation. This objective of this demonstration was to gather information to support the validation of assumptions and resolution of uncertainties with respect to the direct vitrification process. This was accomplished by gather and analyzing data for a material balance around the melter, characterization of the operation of the melter system, and measurement of energy balance data.

EXECUTIVE SUMMARY

Sodium-bearing waste (SBW) is the acidic, high-nitrate liquid product from years of decontamination, laboratory activities, and fuel-storage activities at the Idaho National Engineering and Environmental Laboratory (INEEL). The Batt Settlement Agreement[1] requires that SBW be removed from its storage tanks by 2012. Direct vitrification is being considered as an immobilization method for SBW.

An 8 day, 173 hour vitrification demonstration was conducted using simulated tank WM-180 waste. This demonstration produced 546 kgs of glass at an average rate of 350 kg/m^2/day (rate varied from 325 to 550 kg/m^2/day) using the SBW-9 formulation (30% waste loading on a dry, non-volatile oxide basis). The glass met all product and processing requirements.

In addition, the melter system, comprised of the existing Envitco EV-16 melter system and additional items including plenum heating and a slurry feed system, operated within expectations. No feed system or feed rheology issues were evident. There were some difficulties in feed carryover into the offgas system and other accretions causing offgas system blockage. Also, due to the oxidized nature of the glass (insufficient sugar reductant in the feed), the Molybdenum electrodes and drain were oxidized and eroded beyond acceptable expectations. These issues did not impede accomplishment of test objectives.

The main test objective was to gather data to support a material balance around the melter unit operation. Multiple glass, feed, scrub solution, and filtered solids samples were taken and analyzed. Online offgas monitoring was performed and several manual offgas samples were taken in accordance with EPA methods. These analyses and their evaluation allowed for 83% of the material (not considering nitrate and water that were subject to reactions not otherwise measured) to be accounted for through the duration of the demonstration. Some notable elements, especially Cesium, were not accounted for such as to allow for quantitative determination of their partitioning coefficients.

Energy balance data were also gathered and evaluated. The energy input requirement for this demonstration was 2.54 MWhr/mton/day. It is important to note that the EV-16 melter operates with a water cooled cooling jacket around the refractory, which, in this demonstration, drew 62% of the energy input. Subtracting the cooling water, the energy input requirement was 0.95 MW·hr/mton/day.

A molten salt layer, comprised mainly of sodium sulfate salt, did accumulate over the demonstration period. While this was a departure from crucible tests and laboratory scale melter tests with this same formulation, a one to one comparison cannot be made. These data cannot be compared because the feed material used for this demonstration was found to contain 26% more elemental sulfur than the targeted value. The total amount of sulfate salt mined from the

melter (535 grams) can be accounted for by this extra material. However, is it not appropriate to assume that no sulfate salt would have been observed under target conditions, as some salt have been observed in prior testing with this formulation.

In all, this tested provided data to lead toward the resolving of many of the uncertainties associated with the vitrification of SBW. More testing is required to not only gather additional data not measured in this demonstration, but also to add certainty to the data gathered by showing the repeatability of results. The upcoming EV-16 melter test will endeavor to accomplish these objectives and to leverage the lessons learned from this demonstration.

ACKNOWLEDGEMENTS

The authors would like to acknowledge the following people:

- David Bennert and Rob Wilson from Innovatech Services for invaluable test support and technical input.
- John Hardin, Lee Terry, Rodney Merck, Tim Pruett, and Don Erich at Clemson University for testing support.
- Tanks Focus Area, especially Bill Holtzscheiter and Doug Witt (SRTC) for guidance and direction,
- Jim Rindfleisch, Chris Musick, Arlin Olson, Lance Lauerhass, Charles Barnes, Wes Gamett, Jeff Laug, Ken Brewer, Greg Park, Carol Gies, Brenda Boyle, Duane Lundholm (INEEL), John Vienna (PNNL), and David Peeler (SRTC) for technical support and insight,
- Sharla Mickelson, Shanna Casper, and Natasha Diers (INEEL) for making the report come together,

as well as the funding sources of the DOE-EM program and the Office of Science and Technology.

CONTENTS

ABSTRACT III

EXECUTIVE SUMMARY IV

ACKNOWLEDGEMENTS VI

1. INTRODUCTION 1

2. TEST OBJECTIVES & EXPERIMENTAL APPROACH 1

3. EXPERIMENTAL SETUP & PROCEDURES 2

3.1 WASTE COMPOSITION 2

3.2 FORMULATION 4

3.3 REDOX CONDITIONS 7

3.4 PREPARATION OF MELTER FEED 7

3.5 TEST METHODOLOGY 8

3.6 FACILITY DESCRIPTION 8

3.6.1 Melter System 9
3.6.2 Slurry Feed System 12
3.6.3 Offgas Treatment System 12

4. OPERATIONAL RESULTS 14

4.1 DESCRIPTION OF NOMINAL OPERATING CONDITIONS 14

4.1.1 Feed System Operation 14
4.1.2 Feeding Rate and Melting Rate 15
4.1.3 Melter Operation 16

4.2 OFF-NORMAL CONDITIONS 16

4.2.1 Slurry Feed Pump Vibration 17
4.2.2 Electrode Wear and Electrical Issues 17
4.2.3 Molten Sulfate Salt Accumulation 19
4.2.4 Glass Pour Control 20
4.2.5 Off-Gas Obstructions Due to Salt/Material Accretions 20

5. MELTER PRODUCT CHARACTERIZATION 23

5.1 GLASS VISCOSITY 23

5.2 GLASS DURABILITY 25

5.3 LIQUIDUS TEMPERATURE 26

5.4 PHASE SEPARATION 27

5.5 REDOX RESULTS 28

5.6 SECONDARY WASTE CHARACTERIZATION 31

5.6.1 Solids Condensed in Offgas Lines 31
5.6.2 Solids Filtered from Scrub Solutions 33
5.6.3 Salt Layer on Melter Surface 34

5.7 OFFGAS CHARACTERIZATION 35

5.7.1 Offgas Flowrate and Composition 36
5.7.2 Melter Offgas Flow Rate and Conditions 45
5.7.3 Film Cooler Outlet Offgas Flow Rate and Conditions 45
5.7.4 Melter Offgas Composition 46
5.7.5 Film Cooler Outlet Offgas Composition 47
5.7.6 Film Cooler Outlet Particulate Matter and Metals Measurements 47
5.7.7 Film Cooler Outlet Volatile Organic Compound Measurements 51
5.7.8 Size and Characteristics of Particulate Matter 52

6. MATERIAL BALANCE 56

6.1 OVERALL MATERIAL BALANCE 56

6.2 STEADY-STATE MATERIAL BALANCE 59

6.3 ISOKINETIC SAMPLE TRAIN MATERIAL BALANCE 59

6.4 FATE OF PARTICULAR SPECIES 61

6.4.1 Fate of Sulfur 61
6.4.2 Fate of Nitrogen 62
6.4.3 Water Balance 62
6.4.4 Fate of Cesium 63
6.4.5 Fate of Halides 63

7. ENERGY BALANCE 63

7.1 SUMMARY ENERGY BALANCE 63

7.2 BASES OF CALCULATIONS 64

7.2.1 Electric Power Input 64
7.2.2 Net Chemical Reactions 64

7.3 EVAPORATION OF WATER 65

7.4 HEATING OF GASES IN PLENUM 65

7.5 HEATING OF GLASS 65

7.6 SOURCES OF ERROR 65

8. CONCLUSIONS AND RECOMMENDATIONS 66

8.1 WASTE LOADING 66

8.2 MATERIAL BALANCE 66

8.3 SUPPORT OF THE DESIGN BASIS 67

8.4 RECOMMENDATION FOR FUTURE WORK 69

8.4.1 Molten Salt Formation/Accumulation 69
8.4.2 Changes in Melter Setup to Increase Data Certainty 69

9. REFERENCES 70

APPENDIX A – BATCH SHEETS

APPENDIX B – LOG BOOKS

APPENDIX C – DESCRIPTION OF POST-TEST MELTER MINING

APPENDIX D – ENTROPY INC. OFFGAS SAMPLING REPORT

APPENDIX E – DAS DATA

APPENDIX F – ENERGY BALANCE CALCULATIONS

APPENDIX G – ANALYTICAL DATA

APPENDIX H – INEEL REDOX METHOD

APPENDIX I – MATERIAL BALANCE CALCULATIONS

APPENDIX J – LOG SHEETS

FIGURES

3.1 Impact of sugar addition on glass redox (SBW-9). 8

3.2 Envitco EV-16 melter and slurry feed system 11

3.3 Envitco EV-16 melter and integrated offgas treatment system 13

4.1 Feeding rate over the demonstration period 15

4.2 Melter box with drain, 3 electrodes, and thermocouple rod 18

4.3 Close-up on front electrode that is not visible in Figure 4.2 18

4.4 View of blockage in melter outlet piping 21

4.5 Film cooler exit showing transition from solid to powder accretions 22

5.1 Temperature-viscosity profiles for two glass samples 24

5.2 Secondary electron (or backscatter electron) micrograph and energy dispersive spectrum photo of a molybdenum nodule 28

5.3 Redox ratio (INEEL method) of glass versus melter turnovers....29

5.4 Large agglomerated particles of bulk PM captured in a cyclone....53

5.5 Angular particles, rods, and some cenospheres captured in a cyclone 53

5.6 Rod of condensed, crystalline PM showing hexagonal crystal structure (captured in a cyclone)....54

5.7 This view shows a pentagonal or hexagonal rod, smaller rods, angular particles, and a cenosphere (captured in a cyclone)....54

5.8 PM captured on a filter downstream of the cyclone contains more smaller-diameter rods (~0.3 micron or less in diameter), small ~0.3 micron or less particles, and cenospheres (that are less dense and more easily transported from the cyclone) 55

5.9 A magnified view of a cenosphere and submicron particles captured downstream of the cyclone on a filter suggests some surface layering of condensed material....55

TABLES

3.1 Tank WM-180 Liquid Waste Composition (cations and anions). 3

3.2 Radionuclide Content of Liquid Waste in Tank WM-180.... 4

3.3 Constraints used in SBW glass formulation. 5

3.4 Frit composition.... 6

3.5 Target glass composition (SBW-9). 6

3.6 Refractory composition and properties.... 10

4.1 Operating parameters for FY-01-1 EV-16 melter demonstration.... 14

5.1 Viscosity glass sample composition target and measured values.... 24

5.2 Measured viscosity and temperature values 25

5.3 PCT glass sample composition target and measured values.... 25

5.4 Normalized PCT Release Values (based on targeted compositions).... 26

5.5 Normalized PCT Release Values (based on analyzed compositions) 26

5.6 PNNL redox measurements and comparison to INEEL measurement of same samples 30

5.7 Offgas condensed solids composition 31

5.8 XRD results for condensed solids..... 32

5.9 Composition of filterable offgas solids..... 33

5.10 XRD results for offgas filterable solids 34

5.11 Chemical composition of salt layer mined off melter surface 35

5.12 Melter outlet offgas flowrates and temperatures 37

5.13 Film cooler outlet offgas flowrates and temperatures 38

5.14 Offgas composition at the melter outlet..... 39

5.15 Offgas composition at the melter outlet continued..... 40

5.16 Offgas composition at the film cooler outlet 42

5.17 Offgas composition at the film cooler outlet continued 43

5.18 Particulate and acid gas (Method 0050) measurements at the film cooler outlet 48

5.19 Metals (Method 0060) measurements at the film cooler outlet 49

5.20 Film cooler outlet Summa canister measurements 51

5.21 PM characteristics..... 52

5.22 Estimated particle size distribution for EV-16 particulate matter at the film cooler outlet 52

6.1 Overall material balance and closure value for each measured element (Based on ICP and IC analytical results)..... 58

6.2 Steady-state material balance and closure value for each measured element..... 60

6.3 Isokinetic samples material balance and closure value for each measured element..... 61

6.4 Percentage of elemental sulfur in glass samples versus analyzed feed targets..... 62

7.1 Summary energy balance..... 64

7.2 Energy from chemical reactions 65

8.1 Correlation of test results with technical baseline database 67

Test Results from SBW-FY01-PS-01 Vitrification Demonstration of Sodium Bearing Waste Simulant Using WM-180 Surrogate

1. INTRODUCTION

For about four decades, radioactive wastes have been collected and calcined from nuclear fuels reprocessing at the Idaho Nuclear Technology and Engineering Center (INTEC), formerly Idaho Chemical Processing Plant (ICPP). Over this time span, secondary radioactive wastes have also been collected and stored as liquid from decontamination, laboratory activities, and fuel-storage activities. . . These liquid wastes are collectively called sodium-bearing wastes (SBW). About 3.76 million liters of these wastes are temporarily stored in stainless steel tanks at the Idaho National Engineering and Environmental Laboratory (INEEL). The Batt Settlement Agreement was established in August 1995 between the U.S. Navy, the State of Idaho, and the U.S. Department of Energy (DOE)[1]. One of the requirements per this agreement is to remove SBW from the storage tanks by the end of 2012. To that end, the INEEL is pursuing direct vitrification (no or minimal feed conditioning prior to vitrification) of SBW as the baseline method for immobilizing the waste for long term storage.

The U.S. DOE Office of Science and Technology (through the Tanks Focus Area) and the Office of Waste Management (through the INEEL High-Level Waste Program) are sponsoring a joint effort by INEEL, Pacific Northwest National Laboratory (PNNL), and Savannah River Technology Center (SRTC) to investigate direct vitrification. Testing is being conducted at the Clemson Environmental Technologies Laboratory (CETL) utilizing the EV-16 pilot scale melter as the test bed. This report documents the results of the most recent demonstration conducted in April 2001.

2. TEST OBJECTIVES & EXPERIMENTAL APPROACH

The objective of this pilot scale melter testing, as stated in the Technical Task Plan (TTP), is "focused on maximizing waste loading and obtaining operating data to support the generation of a melter system material balance." The April test was performed on a simulated feed consisting of 30% (dry, non-volatile, oxide basis) WM-180 simulated tank waste and the glass forming chemicals formulation SBW-9 as described by Peeler et al. (2001). This waste loading was chosen as the maximum loading for SBW-9 additive composition that would produce a glass compatible with the waste chemistry while meeting the processing and glass product requirements described in section 5. The glass product requirements are critical both to the disposition of the final waste form in an acceptable long-term storage facility. Furthermore, it is necessary to show that the normal operation of a vitrification system within given parameters is compatible with the glass material. In addition, multiple samples of the feed, glass, and scrub solution were taken during operation. These operating data, combined with on-line and isokinetic offgas sample data, provide the basis for the melter system material balance.

Other data were gathered during the demonstration to support operations assessments and the energy balance. These data were consistent with the objectives laid out in the Test Plan[6]. These objectives included:

- Process Demonstration and Characterization – data are required to verify the feasibility of vitrification of SBW at these processing and waste loading targets. Observations that support this objective include:

- Melting Characterization: Process observations will be made of the melting characteristics of the feed blends presented to the melter. These data provide an indication of the presence of phase separation/salt formation; reductant efficacy, melting reaction kinetics, feed distribution/coverage, degassing/foaming tendencies, and other process characteristics best described through visual observation.

- Construction Material Performance: Observations and measurements will be recorded to assess the relative performance of the refractory, electrodes, and other construction materials used in the melter. These data provide a reference for performance, though are not intended to provide absolute data on refractory or electrode life. Specific items of interest include impact of salts on refractory, electrodes, plenum and heating elements robustness against corrosion. Due to the short duration of the tests, these observations serve to indicate areas for additional investigation.

- Feed Batching and Handling: Feed blending, feed homogenization, and other feed characteristics will be quantified and observed. Flow tendencies, phase separation, and feed agglomeration provide a basis for handling/batching requirements and evaluation of alternative handling systems.

- Melter/System Operations Characterization: Melter operations data will be recorded to provide a basis for developing melter specification requirements for treatment of the actual SBW. These data will be used to identify key design features required of the SBW melter, feed system, and offgas treatment system.

- Offgas Characterization: The offgas produced during the vitrification of the SBW simulant will be measured, sampled and analyzed to quantify the flow rate, process conditions, and chemical composition. The data provide for an initial identification of the key characteristics required for design of the full-scale treatment system.

- Energy Balance - Energy data will be recorded and analyzed to quantify the melting/mixing energy, offgas energy losses, and equipment/process energy losses. Due to the scale of the demonstration system, these data serve only as an indication of the processing performance.

The balance of this report will describe the materials and facilities used in this demonstration, as well as the results of the demonstration and how they impact the test objectives, and what further testing effort is required to realize the goals of the development program.

3. EXPERIMENTAL SETUP & PROCEDURES

3.1 Waste Composition

WM-180 SBW is a strongly acidic (1.008 M H^+ [8]) salt solution. The tanks designated for vitrification are being consolidated into three existing tanks (WM-180, WM-188 and WM-189). No additions or transfers from Tank WM-180 are expected between now and the time of processing. . Thus, the composition in WM-180 is expected to remain the same between now and the time of processing, apart from radionuclide decay. The remaining SBW from other tanks is being concentrated by evaporation and consolidated into tanks WM-188 and WM-189. Tank WM-180 has been sampled and characterized[8]. These factors lead to the choice of a surrogate of WM-180 as the subject of this demonstration.

The WM-180 concentrations used in the preparation of the surrogate for this demonstration are given in Tables 3.1 and 3.2. An explanation for the difference between the "uncorrected" composition that was used and the actual tank characterization is given in Christian[8].

Table 3.1. Tank WM-180 Liquid Waste Composition (cations and anions).

Uncorrected Analytical Results Metals – Average of Mixed & Settled Samples					
Analyte	**Units**	**Value**	**Atomic Wt**	**Molar**	**Oxide %**
TDS	g/L	366.57			
Sp.Gr.@25/4		1.2531			
Acid, Normal	Molar	1.099E+00		1.101	
Aluminum	ug/L	1.70E+07	26.981538	6.28E-01	27.90%
Antimony	ug/L <	7.33E+03	121.757	6.02E-05	
Arsenic	ug/L	3.53E+04	74.9216	4.71E-04	0.04%
Barium	ug/L	7.23E+03	137.327	5.26E-05	0.01%
Beryllium	ug/L	6.61E+01	9.0122	7.33E-06	0.00%
Boron	ug/L	1.26E+05	10.811	0.0116	0.35%
Cadmium	ug/L	8.00E+04	112.411	7.12E-04	0.08%
Calcium	ug/L	1.82E+06	40.0780	0.0453	2.21%
Cerium	ug/L	6.25E+03	140.1160	4.46E-05	0.01%
Cesium	ug/L <	9.70E+02	132.9054	7.30E-06	0.00%
Chromium	ug/L	1.65E+05	51.9961	0.00316	0.21%
Cobalt	ug/L	1.07E+03	58.9332	1.82E-05	0.00%
Copper	ug/L	4.18E+04	63.546	6.57E-04	0.05%
Gadolinium	ug/L	2.63E+04	157.25	1.67E-04	0.03%
Iron	ug/L	1.15E+06	55.845	0.0205	1.43%
Lead	ug/L	2.56E+05	207.2	0.00123	0.24%
Lithium	ug/L	2.22E+03	6.941	3.20E-04	0.00%
Magnesium	ug/L	2.76E+05	24.305	0.0113	0.40%
Manganese	ug/L	7.31E+05	54.9380	0.0133	1.01%
Mercury	ug/L	3.83E+05	200.590	0.00191	0.36%
Molybdenum	ug/L	1.75E+04	95.94	1.82E-04	0.02%
Nickel	ug/L	8.15E+04	58.6934	0.00139	0.09%
Niobium	ug/L <	1.36E+03	92.9064	1.47E-05	
Palladium	ug/L <	2.36E+03	106.4200	2.21E-05	
Phosphorous	ug/L	4.01E+05	30.9738	0.0130	See Phosphate
Potassium	ug/L	7.25E+06	39.0983	0.185	7.60%
Ruthenium	ug/L	1.19E+04	101.07	1.18E-04	0.01%
Selenium	ug/L <	1.09E+04	78.96	1.38E-04	
Silicon	ug/L <	8.00E+00	28.0855	2.85E-07	
Silver	ug/L <	5.38E+02	107.8680	4.99E-06	
Sodium	ug/L	4.47E+07	22.98977	1.94	52.42%
Strontium	ug/L	9.85E+03	87.62	1.12E-04	0.01%
Sulfur	ug/L	2.11E+06	32.066	0.0659	See Sulfate
Thallium	ug/L <	7.89E+03	204.383	3.86E-05	
Tin	ug/L <	4.60E+03	118.71	3.88E-05	
Titanium	ug/L	2.61E+03	47.867	5.45E-05	0.00%
Uranium	ug/L	7.55E+04	237.534	3.18E-04	0.08%
Vanadium	ug/L <	4.44E+04	50.9415	8.71E-04	
Zinc	ug/L	6.48E+04	65.39	9.90E-04	0.07%
Zirconium	ug/L	5.45E+03	91.224	5.97E-05	0.01%

Uncorrected Analytical Results Anions – Average of Mixed & Settled Samples					
Analyte	**Units**	**Value**	**Atomic Wt**	**Molar**	**% in Oxides**
Chloride	ug/mL	1.007E+03	35.4527	0.0284	0.86%
Fluoride	ug/mL	8.700E+02	18.998403	0.0458	0.13%
Nitrate	M	4.8195	62.00494	4.82	
Phosphate	mg/L	1228.2	94.971362	0.0129	0.80%
Sulfate	ug/mL	4.900E+03	96.0636	0.051	3.56%
Sulfate corrected to S		6333.1	96.0636	0.0659	
Iodide(estd)	M	0.0159	126.90447	1.26E-04	0.01%

Table 3.2. Radionuclide Content of Liquid Waste in Tank WM-180

Sample Radioactive Constituent					
		Mixed	**Settled**	**Average**	**g/L**
Am-241	dps/mL	3.22E+03	2.90E+03	3.06E+03	2.56E-05
Co-60	dps/mL	2.05E+02	2.18E+02	2.12E+02	5.81E-09
Cs-134	dps/mL	4.43E+02	4.07E+02	4.25E+02	6.80E-09
Cs-137	dps/mL	1.08E+06	1.15E+06	1.11E+06	3.40E-04
Eu-154	dps/mL	2.36E+03	2.18E+03	2.27E+03	2.40E-07
I-129	dps/mL	8.86E-01	0	4.43E-01	7.27E-05
Np-237	dps/mL	1.65E+01	1.66E+01	1.66E+01	6.73E-04
Pu-238	dps/mL	2.17E+04	2.29E+04	2.23E+04	3.73E-05
Pu-239	dps/mL	3.22E+03	3.36E+03	3.29E+03	1.52E-03
Strontium(total)	uCi/mL	2.28E+01	8.37E+00	1.56E+01	9.56E-05
Tc-99	dps/mL	3.05E+02	3.89E+02	3.47E+02	5.86E-04
Tritium	uCi/mL	2.05E-02	2.32E-02	2.19E-02	6.47E-14
U-234	dps/mL	40.3	38.9	3.96E+01	1.82E-04
U-235	dps/mL	1.16	1.76	1.46E+00	1.94E-02
U-236	dps/mL	2.26	2.06	2.16E+00	9.56E-04
U-238	dps/mL	0.908	0.824	8.66E-01	7.38E-02
Zr-95	dps/mL				0.00E+00
Gross beta	dps/mL				

Note that in the simulated waste the radioactive isotopes of Cesium and Strontium found in SBW were replaced by non-radioactive isotopes. This eliminated the handling of any radioactive material during the testing while maintaining the emphasis on the test objectives. Also, the concentration of the cold Cesium was increased to allow for the concentrations of Cesium in the feed, glass, and secondary waste stream materials to exceed the lower detection limit of the wet chemical analyses. This was necessary to provide enough information for material balance calculations.

3.2 Formulation

Development of a suitable glass formulation was based on defined product and process requirements. Testing was performed to define a suitable glass formulation incorporating the WM-180 simulant based on uncorrected concentrations (Peeler et. al 2001) at a desirable waste loading while still meeting performance objectives. The product performance goals for the glass are described in section 5. These goals were based on a more stringent limit than the Environmental Assessment (EA) glass that is the standard for glass that is considered acceptable at the national geologic repository[9]. Additional constraints were also imposed to ensure that the glass was processable in a reference joule heated melter utilizing Inconel electrodes, and these constraints are given in Table 3.3.

Table 3.3. Constraints used in SBW glass formulation.

Property	Property Limit
η at 1150°C	$2<\eta<10$ Pa·s
Liquidus Temperature (T_L)	$T_L \leq 1050$°C
PCT boron release (r_B)	$r_B < 1$ g/m^2
PCT sodium release (r_{Na})	$r_{Na} < 1$ g/m^2
PCT lithium release (r_{Li})	$r_{Li} < 1$ g/m^2
Salt Layer Accumulation	Unacceptable
Homogeneity	Homogeneous[(a)]

(a) Homogeneity was judged by the lack of second-phase identification by X-ray diffraction [XRD] (as described above) and by optical microscopy at magnifications of ≥ 100×.

As described by Peeler et al[3], a total of ten glass additive formulations, here after referred to as frits (although not actually fritted during glass formulation testing or in subsequent melter tests), were tested by three methods. Dry oxides, carbonates, and single charge liquid melts were used to understand the impacts of various parameters (such as sulfate partitioning) on glass properties and melting behavior and ensure that glass properties requirements were achieved. Each frit was combined with varying amounts of SBW simulant to make glass samples with 25% - 45% SBW waste loading (dry, non-volatile, oxide basis). The performance goals in Table 3.3 were used to select the formulation. The recommended glass composition was based on frit formulation SBW-9. The compositions of the frit are shown in Table 3.4.

Table 3.4. Frit composition.

Oxide	SBW-9 Frit
SiO_2	65.00
B_2O_3	15.00
Li_2O	5.00
Fe_2O_3	10.00
CaO	5.00
Total	100.00

Table 3.5 shows the contributions of waste and frit to the final glass composition (oxide basis).

Table 3.5. Target glass composition (SBW-9).

Element	Oxide	Nominal Weight Percent of Oxide in Glass	Target Weight Percent of Oxide (including substitutions, increases)
SBW Simulant Components			
Aluminum	Al_2O_3	8.40 %	8.27 %
Arsenic	As_2O_3	0.01 %	0 %
Barium	BaO	(Trace)* 0.00 %	0 %
Beryllium	BeO	(Trace) 0.00 %	0 %
Boron	B_2O	0.06 %	0.413 %
Cadmium	CdO	0.02 %	0 %
Calcium	CaO	0.67 %	0.67 %
Cerium	Ce_2O_3	(Trace) 0.00 %	0.00198 %
Cesium	Cs_2O	(Trace) 0,00%	0.0591 %
Chromium	Cr_2O_3	0.06 %	0.0621 %
Cobalt	Co_2O_3	(Trace) 0.00 %	0 %
Copper	CuO	0.01 %	0.0135 %
Gadolinium	Gd_2O_3	0.01 %	0.00783 %
Iron	Fe_2O_3	0.43 %	0.423 %
Lead	PbO	0.07 %	0 %
Lithium	Li_2O	(Trace) 0.00 %	0 %
Magnesium	MgO	0.12 %	0.118 %
Manganese	MnO	0.25 %	0.299 %
Molybdenum	MoO_3	0.01 %	0.00676 %
Nickel	NiO	0.03 %	0.0268 %
Potassium	K_2O	2.29 %	2.25 %
Ruthenium	RuO_2	(Trace) 0.00 %	0.00404 %
Sodium	Na_2O	15.78 %	15.5 %
Strontium	SrO	(Trace) 0.00 %	0.00301 %
Titanium	TiO_2	(Trace) 0.00 %	0 %
Uranium	U_3O_8	0.02 %	0 %
Zinc	ZnO	0.02 %	0.0208 %
Zirconium	ZrO_2	(Trace) 0.00 %	0 %
Chloride	Cl	0.26 %	0.260 %
Fluoride	F	0.17 %	0.225 %
Iodide	I	(Trace) 0.00 %	0.0415 %
Phosphate	P_2O_5	0.24 %	0.237 %

Sulfate	SO_3	1.07 %	1.05 %
SBW Simulant Waste Loading in Glass		**30.00%**	**30.0 %**
		Glass Formers	
Boron	B_2O_3	10.50 %	10.5 %
Calcium	CaO	3.50 %	3.50 %
Iron	Fe_2O_3	7.00 %	7.00 %
Lithium	Li_2O	3.50 %	3.50 %
Silicon	SiO_2	45.50 %	45.5 %
Glass Formers in Glass		**70.00 %**	**70.0 %**

[*] Trace components are present in the glass at weight fractions on the order of 10^{-5} or less.

3.3 Redox Conditions

As WM-180 SBW contains 4.82 M nitrate, it is a strongly oxidizing solution. It is desirable, however, to operate the pilot-scale melter at CETL under moderately reducing conditions, (0.2-0.3 Fe^{2+}/Fe_{total} based on previous experience with this melter and Mo electrodes[5]). The lower constraint was established to avoid oxidation of the Molybdenum electrodes that were installed in the EV-16 melter at the time of the demonstration. The upper limit was set to avoid undesirable reduction of the oxides in the glass to form metal precipitates that could lead to increased electrical conductivity and short-circuiting. The benefit of chemical reduction versus thermal reduction of the nitrate was important to achieving desirable melting rates and minimizing foaming. Since iron is a significant component in the glass, it can be used as a measure of the redox condition of the glass. Specifically, the ratio of ferrous (Fe^{2+}) iron to total iron content in the glass is the parameter of interest.

To reduce nitrate in the feed and some iron in the glass a reducing agent is added to the feed formulation. For this test, sugar was chosen as the reductant additive. A parallel effort (with respect to activities preparatory to the demonstration {post-formulation}) including laboratory tests developed the relationship between sugar to nitrate ratio in the feed and the redox state of the glass[20]. The laboratory tests were performed using slurry fed crucibles in a furnace that was at the desired glass melt temperature. That relationship is shown in Figure 3.1. Because a Fe^{2+}/Fe_{total} ratio of 0.2 was desired, sugar was added to the feed slurry at 160 grams per liter, equivalent to a sugar to nitrate ratio of 31 grams sugar per mole nitrate. This value was chosen not because it was predicted to exactly reach a redox ratio of 0.2, but rather because the feed system conditions allowed for easier addition of sugar in the event of a lower redox ratio that for a decrease in the sugar/nitrate ratio in the event of too high a redox ratio.

3.4 Preparation of Melter Feed

The SBW contains high concentrations of metals ions in solution. To keep some of these metals from precipitating during preparation of the simulant, a detailed recipe was developed by Christian (2001). Most metals were added as nitrate salts. Some reagents were prepared as separate solutions before addition to the bulk simulants. A batch sheet that combines the steps in the recipe with the calculations for the appropriate masses and volume of reagents was developed for the test. A copy of a generic batch sheet, along with specific batch sheets and the recordings of the amounts of feed added are found in Appendix A.

Figure 3.1. Impact of sugar addition on glass redox (SBW-9).

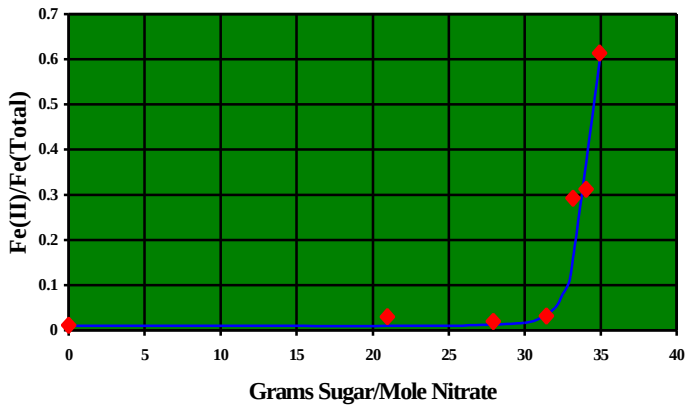

Weeks prior to the demonstration, waste simulant without RCRA metals and glass forming additives were prepared and analyzed. The analysis showed that the major components in the waste, namely Na, Al, K, Mo, NO_3, and total S, were on target (whereas the sulfate content in the feed was shown later to be 20% high, see section 5). Immediately prior to the demonstration, Cd and Ni were added to the waste, rounding out the 30% waste loading formulation.

3.5 Test Methodology

Test methods and procedures were necessary to ensure that the demonstration would meet its stated objectives. These methods and procedures are documented in the test plan[6] and the run plan[10].

The test plan outlined the general objectives of the demonstration and how they would be met in higher-level terms. The run plan contained more step-by-step procedures and methods regarding operating parameter bounds, sampling procedures and frequency, as well as important training and safety information.

3.6 Facility Description

The SBW vitrification demonstration (PS-FY01-1) was conducted at Clemson University's Department of Environmental Engineering and Science (Clemson EES). Both facilities are located at the Clemson Research Park, in Anderson, South Carolina. The melter is installed at the DOE/Industrial Laboratory for Vitrification Research. The laboratory is a controlled-access facility that permits the testing of multiple competing technologies in a single independent site. The site was selected as the test bed for demonstrating vitrification of INEEL wastes based on availability, facility support, environmental permitting, and the established partnership with DOE.

The laboratory at CETL is equipped with the EV-16 melter, as well as other melter technologies suitable for pilot scale testing. The facility is permitted by the State of South Carolina to conduct treatability studies on hazardous waste streams and waste surrogates. The laboratory houses the melters and dedicated offgas treatment systems capable of treating the emissions from liquid feed or dry feed streams. The melters are equipped with the necessary feed systems for slurry or dry feeds.

3.6.1 Melter System

The EV-16 melter system serves as a platform for demonstrating vitrification processes on a variety of waste streams. The melter system is shown in figures 3.2 and 3.3. By design, it offers process flexibility for cold/warm/hot top operations, low and high melting temperatures (less than 1150°C and in excess of 1350°C), slurry or dry feed, and a variety of other test conditions. The data generated through testing of the melter and supporting systems serves to demonstrate the feasibility of direct vitrification of the INEEL SBW. Tests conducted with the EV-16 melter provide valuable information and design data, but do not reflect the optimal melter or process design. Melter selection will require additional testing so that proper attributes can be identified and formal specifications developed for the INEEL SBW.

The melt chamber of the EV-16 is 45.7×45.7 cm, with a design depth of 40.6 cm. The melter is lined with 75 mm of Unicor 501, fused-cast alumina-zirconia-silica (AZS) refractory. The presence of precipitated metals in previous tests led to the installation of a sloped bottom, which was ram formed using a Narco Zirmul 160. The Zirmul 160 is close in composition to the Unicor 501, with slightly lower ZrO_2, offset by higher Al_2O_3 and P_2O_5 bond. The Zirmul 160 was formed to create a concave bottom intended to direct any precipitates to the drain orifice area. In this configuration, the working volume of the melter is approximately 55-L (approximately 143 kg), assuming a freeboard above the melt line of 75 mm. The composition and key characteristics of the Unicor 501 and Zirmul 160 are presented in Table 3.6.

The refractory melt chamber is encased in a shell of segmented water-cooled panels. The water-cooled shell serves as the binding steel for the refractory and provides a connection point for any support hardware or fixtures as necessary. The shell also serves as a safety feature, minimizing the potential for glass leakage in case of a breach in the refractory lining. If excessive wear or damage occurs to the refractory lining of the melter, the water-cooled panels are designed to freeze the molten glass and effectively seal the tank. The cooling shell also provides an additional safety feature by protecting workers from contact burns that could occur through exposure to the outside face of the refractory. This approach is similar to that applied at the Savannah River Site DWPF and the West Valley Demonstration Project.

Table 3.6. Refractory composition and properties.

Composition/Property	Unicor 501	Zirmul 160
ZrO_2	33.75 mass%	25.1 mass%
Al_2O_3	49.00 mass%	56.3 mass%
SiO_2	15.29 mass%	12.5 mass%
Fe_2O_3	0.22 mass%	0.05 mass%
TiO_2	0.17 mass%	0.09 mass%
Na_2O	1.32 mass%	N.D.
Alkali/Alkaline Earth	N.D.	0.12 mass%
P_2O_5	N.D.	5.7 mass%
Others	0.25 mass%	N.D.
bulk density	3.73 g/cm^3	3.15 g/cm^3
Apparent Porosity	1.15%	16%

The melter as supplied by Envitco (Toledo Engineering Company, Inc. [TECO], Toledo, Ohio) was designed for testing cold-top or warm-top melting processes. A modified melter plenum was installed for testing SBW feeds under hot-top conditions prototypic of a full-scale liquid fed ceramic melter. The modified plenum contains $MoSi_2$ elements that penetrate the roof of the melter plenum, and are capable of providing up to 50 kW of heat to the plenum region. Feed, offgas, view port, and video camera penetrations are provided through the four walls of the structure. Access to the melt surface is via one of the wall-mounted ports.

Joule power is applied to the melt bath through a 100-kVA power supply, which uses a Scott-T transformer to convert the three-phase power to a balanced two-phase input to the furnace. The applied power is controlled through two SCR/secondary transformer sets, which are adjusted to the desired power level through a common potentiometer control. Four 32-mm molybdenum electrodes enter the melter horizontally through each of the four sides of the melt chamber. The electrodes are installed through water-cooled holders, thereby allowing the operator to adjust or advance the electrodes in case of wear or process changes.

The power supply is fitted with auto-tap circuitry that maintains the control at an optimum power factor (between 0.92 and 1.0) while operating within the range of any of the three transformer tap zones. The three selectable transformer tap zones, coupled with the adjustable electrode power settings, allows the melter system to process a wide range of glass compositions, temperatures, and resistivities, with the same basic melter, power supply and electrode configuration.

The molten glass is drained from the bottom of the melter through a molybdenum orifice. Flow rates are controlled by adjusting the position of the bottom drain probe relative to the drain orifice. The bottom drain probe consists of an Inconel drain probe mounted on a precision linear slide. Micrometer-controlled positioning allows minute adjustments in drain rate. To facilitate start-up and maintenance activities, the bottom drain probe assembly may be retracted.

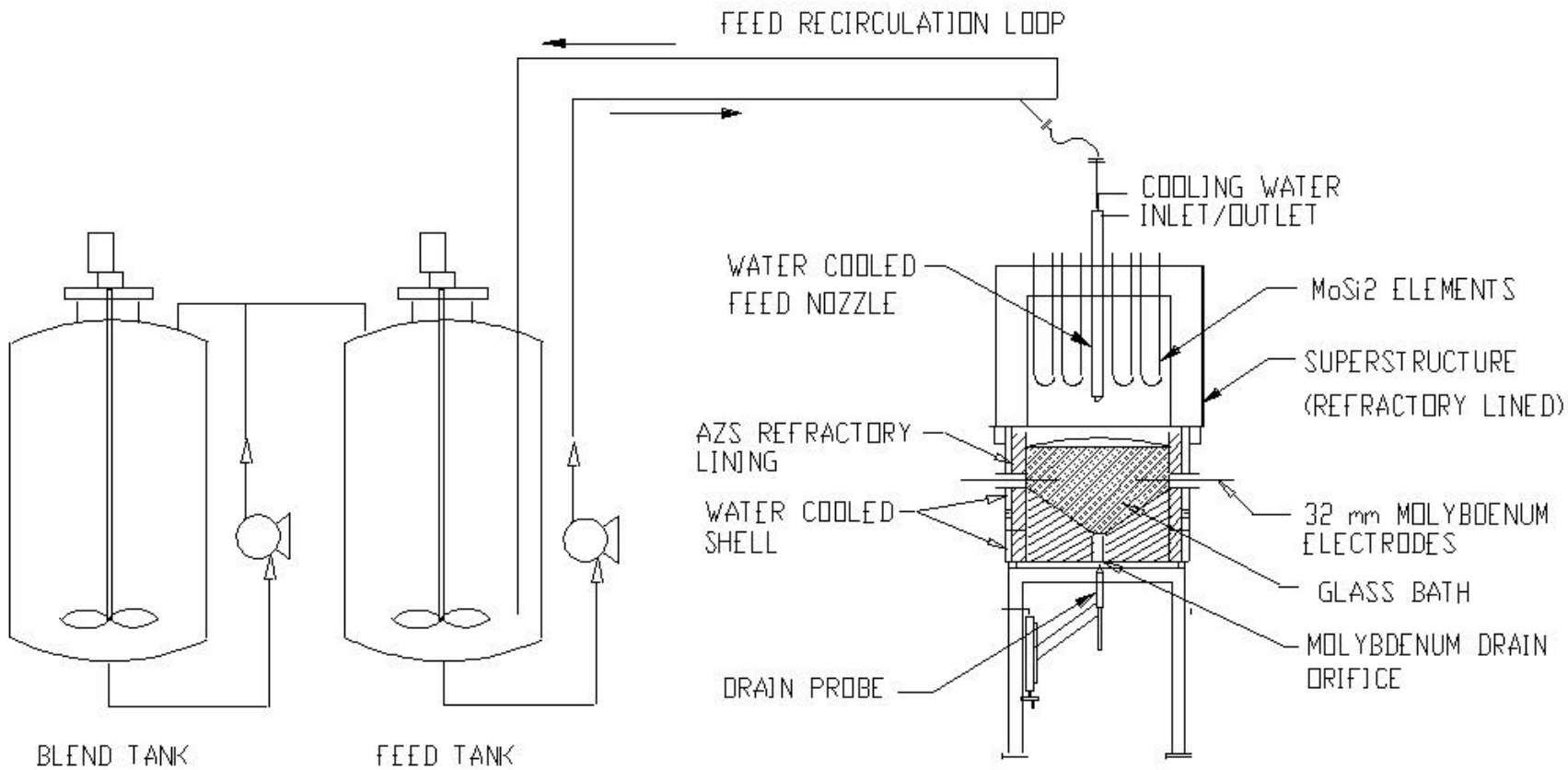

Figure 3.2. Envitco EV-16 melter and slurry feed system.

3.6.2 Slurry Feed System

The slurry feed system consists of a mix tank, feed tank, mix and feed tank transfer and recirculation lines with diaphragm transfer pump, melter feed recirculation line, centrifugal feed pump, and slurry feed nozzle. Each tank is mounted on load cells for batch mixing and feeding rate monitoring. An output signal from the feed tank load cells interfaces with the data acquisition system (DAS) for continuous feed monitoring.

A vertical submersible pump transfers feed from the feed tank to the recirculation line and maintains sufficient fluid velocity to prevent feed components from settling within the recirculation line. Slurry feed is transferred to the EV-16 through a slipstream from the recirculation line. The melter feeding rate is controlled by recirculation line backpressure. Feed is delivered to the center of the melt surface of the EV-16 through a water-cooled slurry feed nozzle penetrating the melter plenum from a port vertically centered above the melt surface.

3.6.3 Offgas Treatment System

The offgas system consisted of a film cooler, quench, air atomizing scrubber, cyclonic separator, packed column, and high efficiency mist eliminatory (HEME). The system is constructed of 304 stainless steel (where temperatures are high) and PVC (where temperatures are low enough). Gases exiting the melter were cooled to by means of the film cooler, which was located approximately 2 feet from the hot face of the melter. Offgas samples were extracted from a port immediately downstream from the film cooler, in a vertical 3 inch inside diameter (ID) duct that was configured to meet the minimum spacings/location requirements for isokinetic sampling systems. The offgas then passed into a quench tower that further cooled the offgas to its dewpoint. The particulate matter (PM) and acid gases are scrubbed in the air atomizing scrubber. This is similar to scrubber system used in the DWPF offgas system, but air is used instead of steam to atomize the scrub solution. Additional scrubbing and aerosol removal is performed in the packed bed, and mist eliminator. The operations from the quench to the packed tower operated at a target neutral (pH=7) scrub solution by adding KOH solution as needed.

Since a heat exchanger was used to cool the recycled scrub solution, the quench unit was not truly adiabatic. Some of the moisture in the offgas was condensed, resulting in an increase over time of the volume of total scrub solution. In an optimized scrubber system, less (or no) water condensation in combination with any makeup water may better optimize the amounts of secondary waste generated from scrub solution blowdown. The offgas treatment system is matched to the EV-16 melter based on its general applicability to a variety of offgas conditions. Optimization of the offgas treatment system design will require additional investigation based on offgas characterization data generated through these tests and future demonstrations.

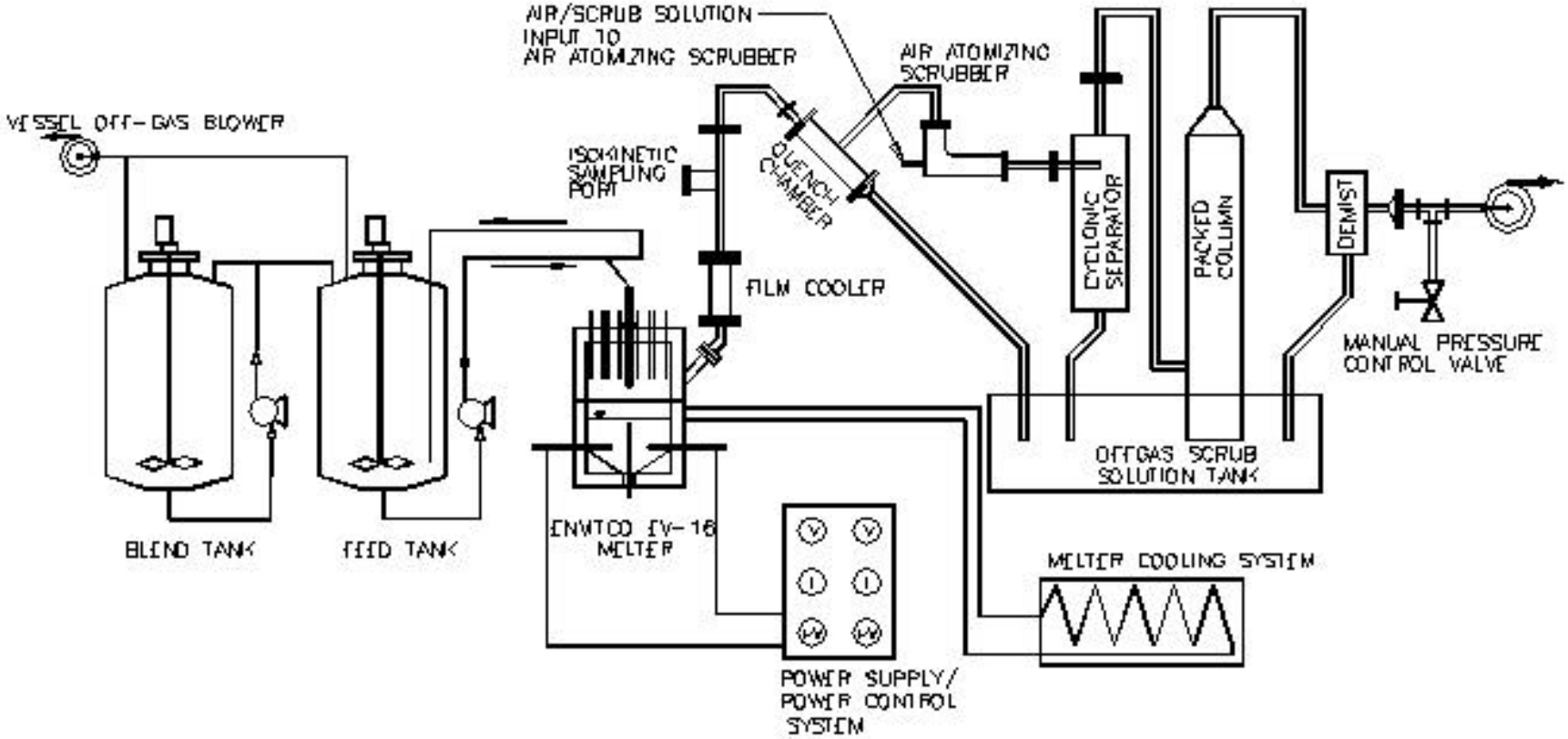

Figure 3.3. Envitco EV-16 melter and integrated offgas treatment system.

4. OPERATIONAL RESULTS

4.1 Description of Nominal Operating Conditions

The April demonstration took place from April 3 through April 11. The melter system was run 24 hours per day with downtime for sampling or system upsets. The operators worked 3 8 hour shifts per day. The demonstration was conducted in accordance with the test and run plans. Table 4.1 describes the key operating conditions chosen based on glass formulation parameters, EV-16 melter system configuration, and the desire to model to scale the conditions likely to be seen in the production model of the waste vitrification facility. The main subsystems' operations are described below.

Table 4.1. Operating parameters for FY-01-1 EV-16 melter demonstration[10].

Parameter	Target
Glass melt temperature, °C	1150
Plenum temperature, °C	600
Plenum pressure, inches of water	-0.5
Air inleakage rate, scfm	30 (estimated)
Total offgas flowrate, scfm (including film cooler)	65 (estimated)

4.1.1 Feed System Operation

The feed system as originally designed was configured to mimic the feed control system employed by DWPF. In this design, the feeding rate to the melter is controlled by adjusting the backpressure on the feed recirculation loop. As the backpressure on the loop is increased, the feeding rate to the melter also increases. The feed system was used in this mode for several hours, but was ineffective due to the lower than expected feed viscosity. Control problems were further compounded by the low melting rate/feeding rates observed in the initial phase of the demonstration.

The feed system was modified to include a peristaltic pump to control the rate at which feed was presented to the melter. The pump was located on the feed takeoff leg and drew feed from that leg to the melter cavity. This methodology allowed the recirculation rate to be kept sufficiently high to avoid particle settling, while maintaining a feeding rate consistent with the observed melting rate.

The peristaltic pump was set to provide the desired feeding rate. The feeding rate was confirmed visually via the closed-circuit TV system focused on the melt surface, and the feeding rate readout as indicated by the Data Acquisition System (DAS) gathering of flowmeter data. Occasionally it was necessary to adjust the feeding rate based upon continuous increase in the cold cap coverage. A high feeding rate caused the liquid feed and cold cap to cover the entire viewable surface, making the picture very dark. A low feeding rate caused a very small liquid pool of feed or small cold-cap to exist with much of the melt surface visible. As explained below, attempts were made to keep the cold-cap and liquid feed pool covering most of the viewable area.

The feed nozzle itself was based on a PNNL slurry feed nozzle design . The nozzle was water cooled and inserted in through the top center of the plenum. Feed was presented approximately seven inches above the melt surface. Unlike in previous tests or with other feed nozzle designs, restarting the feed after some downtime was not problematic. In the event that the feed did not immediately restart, the feed system was equipped with both air and water flushing sources. Administrative controls were placed on the flushing of the feed nozzle, and required that any flushing be done with the nozzle removed from the melter. This was done to avoid potential dangers associated with injection of water into molten salt.

These various parts of the feed system contributed to the maintenance of a feeding rate that was consistent with the observed melting rate.

4.1.2 Feeding Rate and Melting Rate

The observed feeding rate was lower than anticipated based on previous demonstrations (Research Scale Melter (RSM) test RSM-01-1 (Goles et. al. 2001). The nominal feeding rate during the first half of the demonstration was 0.225 L/min, compared with the expected feeding rate of approximately 0.455 L/min, which was predicted based on scaling of the RSM-01-1 melting rate scaled to the EV-16 surface area. Figure 4.1 presents the feeding rates during the demonstration, with downtime removed for simplicity.

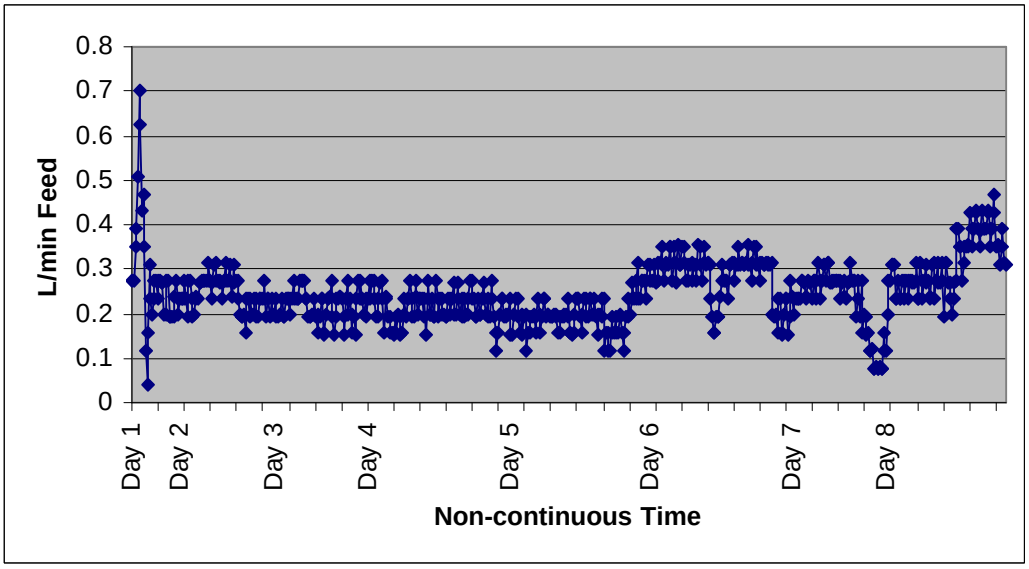

Figure 4.1. Feeding rate over the demonstration period.

The nominal feeding rate was higher over the last 3 days of the demonstration. This is believed to have occurred due to establishment of steady state glass composition (since the increase coincided with the completion of 3 melter turnovers, as well as an observed increase in the amount of molten salt present on the melt surface and an increase of cold-cap coverage. A layer of molten salts is thought to improve heat transfer within the cold cap[12] and has been shown to increase melting rate with similar chemistries and operating conditions (Goles, 2001). A layer of molten sulfate salts was observed during the demonstration.

The feeding rate was established based on observation of the melt pool coverage and by attempting to maintain a consistent cold-cap. As stated, observation of the cold cap was done through the use of a video monitoring system that was focused on the approximately 30-50% of the melt surface. This limited field of view is believed to have made the melt pool coverage seem greater than actual size, which lead to incomplete coverage, lower feeding rates, and hence lower melting rates. This was one of the primary contributors the lower feeding rates observed in the EV-16 test versus the RSM-01-1 test.

As shown in Figure 4.1, the increasing melting rate lead to sustainable feeding rate periods of 0.265 L/min and 0.375 L/min later in the demonstration. This still lagged behind the *average* feeding rate of the RSM demonstration, but was appreciably better than observed in the first days of the test. These feed rates correspond to a range of 380 to 540 kg/m^2/day.

4.1.3 Melter Operation

The melter itself was the primary unit operation of interest during this demonstration. The test plan identified target conditions of its operation based on previous testing, including a previous EV-16 SBW test[18], RSM-01-1 and DWPF operating conditions, and the need to measure process data to support ongoing design activities. Data collection was conducted through both on-line data acquisition and manual monitoring as required. Consistent with Table 4.1, the melter was operated at the target melt temperature of 1150 °C and an offgas exit temperature of 350 °C. .

Melt and plenum temperatures were maintained through controlled power input. The electrodes described in section 3.6 provided joule power input to the glass. Plenum heating was accomplished through a combination of radiant heat transfer from the melt and melt tank walls, as well as through the plenum heating elements. The power input to the energy balance was consumed through heating of the feed materials and related reactions (evaporation, oxidation, mixing), heat loss to the offgas and drained glass, radiant heat loss through the plenum skin, and heat loss to the cooling jackets surrounding the melt chamber and exhaust gasses. These inputs and losses are detailed in section 7.0, Energy Balance.

One of the most critical aspects of the melter operation is the control and maintenance of the cold-cap. Early in the test, when minimal segregated salts were observed on the glass melt, the liquid feed that dropped onto the surface seemed to boil, dry, and form what was observed to be similar to a typical cold-cap. When feed was stopped the liquid feed that was present burned off or incorporated into the cold-cap in a very short time (one minute or less), while the remaining cold-cap then took 3-5 more minutes on average to burn off. After these burn off periods, the melt surface was probed for molten salts. As there were not molten salts present during this period of the tests, this may account for this cold cap behavior differing from the RSM-1 test behavior.

Later in the test, the cold-cap behavior was more like that observed in RSM-1 most likely due to the presence of molten sulfate salts. In the presence of these salts, the cold-cap occupied less area under the ureacted, undried slurry. When feeding was stopped at any given time, the liquid would rapidly disappear, but the remaining cold-cap underneath was much less than noted previously (less than 50% of liquid feed coverage area). This observation is supported by observations recorded in the demonstration log book (Appendix B). The edges of the liquid feed pool appeared foamy, but feed that flowed to the edges of the pool rapidly digested into the melt, with no observable dry cold-cap period. The slight foam that appeared at these edges was soft and flowed easily. It is not clear whether these conditions were caused by the increased presence of molten salts or by the increase in plenum temperature and associated radiative heat transfer, as both of these conditions marked this period. Draining of the melter was performed periodically rather than continuously due to difficulties in maintaining control at the low melting rates. Effort was made to maintain the glass level at ± one inch of target, which was 3 inches below maximum tank level. The periodicity of the pours ranged from hourly to two times per eight-hour shift. Each time the amount of glass poured was intended to match the amount of oxides fed to the melter since the last pour, based on an oxide/feed ratio of 0.20. At least once per shift, the melter was shut down to manually measure and confirm the glass level in the melter.

4.2 Off-Normal Conditions

Both planned and unplanned conditions were experienced during the demonstration. Some unexpected events occurred during the test Several modifications are planned for this system prior to the next planned test to resolve these events.

4.2.1 Slurry Feed Pump Vibration

Mid-way through the demonstration, vibration in the feed tank was noted. The vibration was attributed to the centrifugal recirculation pump mounted in the tank. Initially it was believed that the mixer drive motor or drive system had a harmonic vibration that could be overcome by varying the speed of the pump. Later, this same noise grew more persistent in both frequency and intensity. Following the demonstration, the pump was removed and returned to the manufacturer for evaluation. Disassembly of the housing revealed that the lower Teflon bearings had been entirely worn away, as was the double lip Teflon seals designed to protect the bearing. Though the same design had been used in similar applications, the vendor made several improvements including addition of a second outer seal on each end of the bearing, independent grease lines to each bearing (upper and lower), and increased grease flow rate using a higher capacity automatic grease canister.

4.2.2 Electrode Wear and Electrical Issues

A failed capacitor and control card in the power control unit caused an early termination of the demonstration (test objectives had been met, but it was intended that more feed would be processed). This unit controlled the power to one of the glass electrode zones, in this case Zone 2. Zone 2 was powering the front and rear electrodes of the melter, and was also coupled with the glass drain heating circuit. Figure 4.2 shows an overhead photo of the electrodes. The Zone 2 electrode, which was coupled to the glass drain was about 75% consumed (oxidation/chemical attack) is hardly visible in the photo. In a previous demonstration this electrode had been withdrawn 1.5 inches from the melter to reduce the amperage to the drain circuit. This reduced the surface area available for energy transfer, and likewise, increased the current density specifically for this electrode. Figure 4.3 shows a close-up shot of that electrode.

Figure 4.2. Melter box with drain, 3 electrodes, and thermocouple rod.

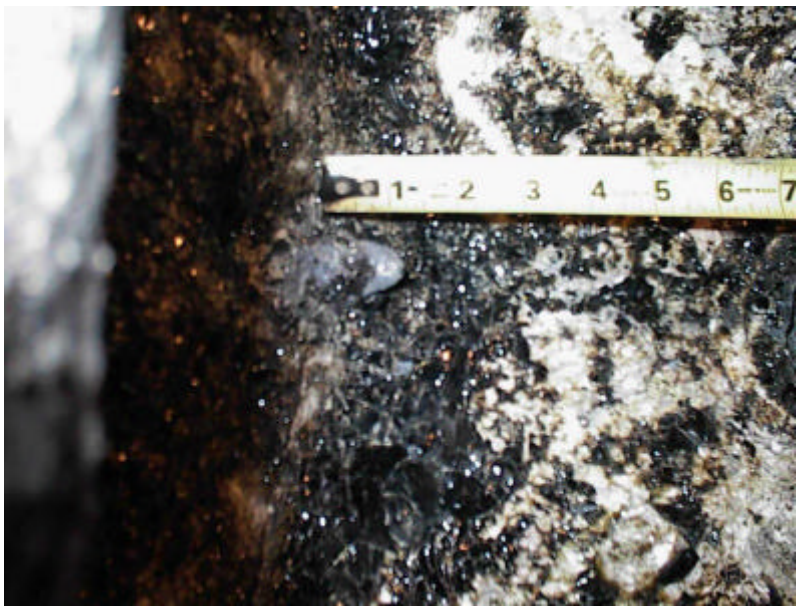

Figure 4.3. Close-up on front electrode that is not visible in Figure 4.2.

Note: Although not applicable as an electrical issue, it is important to point out that no other significant corrosion was evident after mining the melter, as stated in the memo describing the mining of the melter in Appendix C.

Earlier in the test, the Zone 2 control fuse had blown upon a restart of the power. After the fuse was replaced, the glass temperature had dropped to the point that continuity was lost in Zone 2. The preferential loss of Zone 2 is attributable to the short length of the front electrode, and the loss of heat

around the electrode due to its close proximity to the melter wall and water-cooled electrode holder. Continuity was eventually reestablished through gradual re-heating of the melt tank using the plenum heaters and Zone 1 heat.

For the next demonstration, the EV-16 melter is being modified to use Inconel-690 plate electrodes to eliminate this issue.

4.2.3 Molten Sulfate Salt Accumulation

Although molten salt accumulation was not, in and of itself, an operational issue, it did affect the operation of the melter system. Per the test plan, an administrative control was set on the amount of molten sulfate salt that would be allowed to form on the surface of the glass before some action would be taken. Based on calculations patterned after those performed in previous molten salt steam explosion studies[12] the limit was set to approximately 2 cm. This limit was exceeded early in the test, when a discontinuous layer of salt was detected after burning off the cold cap for the purpose of probing for a salt layer (feed analysis results {section X} show that the total sulfate in the feed exceeded the desired amount by 20%, which may offer some explanation as to why the molten salt formed). The method for finding a salt layer and estimating its thickness consisted of manual probing with a cold, dry alumina probe and viewing the length of the probe covered in salt down to the first part of the probe covered in glass. Given the angle of entry of the probe into the melt surface, the thickness of the salt at that point on the surface could be estimated. This method may not provide a totally accurate accounting of the salt presence, as the probe itself may pool the material and cause incorrectly high readings

The salt layer that was first detected after approximately 50 hours ranged from scant at some points to as deep as 1 inch. It should be emphasized that this pocket of salt that was measured did not exist over the entire surface, and the measurement method was not entirely accurate due to reasons stated above. As this measurement exceeded the administrative constraint on salt buildup, a mitigation plan was put into action. Small amounts of a variety of reductants were placed on the melt (salt) surface, including graphite paper, sugar, and polystyrene, while observing the salt reactivity. These materials were either oxidized slowly or gave no indication of preferential reaction with the salt Ground anthracite (69% carbon) was added to the surface and appeared to be reactive in the pockets of salt, while only mildly reactive when placed on the glass surface. It is as yet unclear whether the carbon actually reacted to reduce the salt, as there was little or no increase in SO_2 evolution as indicated by the CEM monitoring, or catalyzed some other reaction. The CEM showed an increase in CO and CO_2 each time a reductant was added, so it is clear some change in the oxygen activity occurred, be it the observed oxidation of the reductant or some reaction in the case of anthracite.

Anthracite was added approximately one time per day. The only quantifiable salt observation was that approximately 525 grams of solid salt, consisting predominantly in sodium sulfate (see analysis in section 5.6), was mined from the top of the melter after the demonstration had been completed and the melter cooled. Other aspects of the fate of sulfur are explained in section 9. The upcoming demonstration planned for September 2001 will be operating with a different glass formulation and a corrected WM-180 composition simulant. The waste loading has been reduced and glass former composition altered to counteract what was perceived to be a lack of adequate sulfate incorporation into the glass, but the feed results do show that 20% more sulfate was fed to the melter than expected, which may account for the molten salt presence in this demonstration of the SBW-9 formulation.

4.2.4 Glass Pour Control

The EV-16 melter, as described in section 3, was designed with a bottom-drain rather than an airlift or teapot spout that is called for in the current baseline WVF melter design. The draining from this orifice is primarily controlled by the temperature of the drain itself, which in turn is controlled by the drain electrode and a combined air/water cooling system. In addition, a secondary mechanical drain control valve has been added. The valve consists of an Inconel plunger which restricts the flow area in method similar to a needle valve. The plunger and probe were very desirable from the perspective of controlling the flow of glass pouring from the melter and stopping the flow at the end of a pour, while the temperature control was mainly used to initiate the glass pull.

During the demonstration, a few events caused the mechanical drain probe system malfunction. Due to the low pour rates, glass would occasionally collect on the side of the probe, making it difficult to seat the drain probe correctly. This problem was mitigated by allowing glass to pour over any glass buildup on the probe, melting and flushing it away prior to reinserting the probe into the orifice. At one point during the demonstration, the accumulation of glass on the probe adhered to the side of the drain housing as the probe was lifted into position. Attempting to remove the probe from the side of the housing bent the probe, requiring manual adjustment and removal/reassembly of the probe assembly.

After 4 days of operation, the wear was noticed in the drain orifice, and was apparent when the drain probe could no longer stop the glass flow without additional cooling of the orifice. The logbook entry for 4/7 at 13:19 indicates that air and water were used to cool the drain to terminate a pour that would not stop using the drain probe. This methodology was employed throughout the rest of the demonstration.

Further inspection of the orifice, minimally during the run and more completely after the run, indicated that the bottom knife-edge had eroded, hence destroying the sealing surface between the drain and the probe. This erosion may also have been exacerbated by oxidation of the orifice, both along the knife-edge as well as through the orifice itself. Given that the glass being poured through the orifice was not quite as chemically reduced as desired (see redox results, section 5.5) in order to avoid oxidation of the Molybdenum, wear to the orifice was likely a combination of oxidation and erosion. In addition, metallic streaks and some nodules were evident in the glass. One of these nodules was analyzed by SEM and found to consist of primarily molybdenum, sodium, and oxygen, indicating perhaps a sodium molybdate. This supports the conclusion that erosion was the prime cause for the lack of mechanical control of the glass pours. The next demonstration (planned for September 2001) will be conducted using only the temperature control system for glass pours, and the drain assembly is being changed to Inconnel to avoid wear attributed to oxidation/reduction control.

4.2.5 Off-Gas Obstructions Due to Salt/Material Accretions

Problems were experienced in the offgas system due to the deposition of entrained material in the ductwork. Within 24 hours of the beginning of the demonstration, large pressure drops were noted in the offgas system, specifically in ductwork between the melter and the quench chamber. The drop in pressure increased with time, which lead to the decision to place the melter in standby and remove the film cooler and associated ductwork for inspection. Throughout the offgas piping, starting at the melter exit, continuing up through the film cooler and riser above film cooler, there were varying types and degrees of deposition.

Upstream of the film cooler, the deposition consisted of unmelted and/or partially melted feed, which tended to form a ceramic accretion on the pipe inside wall with the same coloring (rust to red) as

the feed material. The material was solid and compact, and could only be removed by chipping or grinding; brushing had no affect. Figure 4.4 shows a view of this blockage.

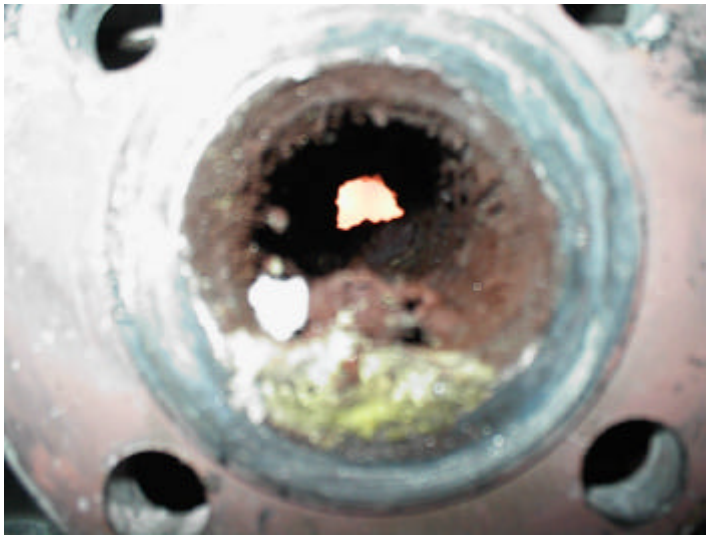

Figure 4.4. View of blockage in melter outlet piping (The light portion in center of picture is the only portion open for flow).

Blockage associated with feed deposition was most prevalent in the 0.6-meter long duct connecting the melter plenum to the film cooler. At this location, before the hot offgas and entrained aerosols is cooled in the film cooler, the hot aerosols adhered to the pipe interior wall. At least some of the aerosols were molten, solidified in the accretion buildup, and caused a very tough deposit. The duct, which was insulated but not heated, was not designed or heated to allow the deposits to remain molten and drain into the furnace. Higher amounts of deposition inside the flanged ends of the duct were attributed to the local temperature drop that occurs in flange area due to increased conduction of heat from the duct through the flange. These local cool zones allowed for material to accumulate in greater amounts than in the rest of the duct, although there was a coating throughout. This plugging could be avoided if the film cooler were placed/coupled to the melter (i.e., avoid the transition run).

Downstream of the film cooler, deposits were predominantly made up of condensed salts, which tended to more of a friable, powder-like consistency. This material would release from the walls by brushing or by tapping the pipe to vibrate the material loose. The photo in Figure 4.5 shows both the powdery material downstream from film cooler as well as the more solid material upstream. This transition demonstrated that the film cooler was helping to make the material more friable, with less chance to agglomerate as the material upstream of the film cooler. Unfortunately, this assistance did not completely prevent downstream blockages.

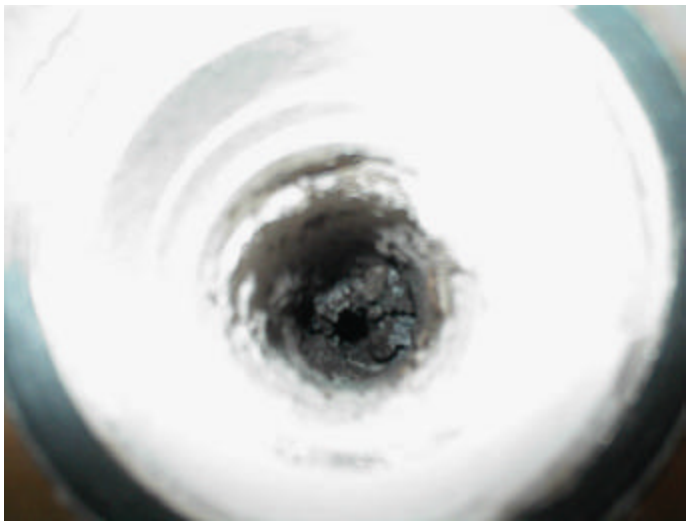

Figure 4.5. Film cooler exit showing transition from solid to powder accretions (dark material are solid, lighter material are powdery).

The riser from the film cooler connects to a 90º elbow and horizontal jumper, which carries the offgas to the quench chamber. The elbow was also a location of particulate matter agglomeration/impaction. The first time the film cooler and riser were dismantled, it was noted that the 2 inch inner diameter pipe had been constricted to less than 1 inch. The horizontal run also contained two more 90° elbows, which were installed in series to bring the offgas line back on center with the quench. Material tended to agglomerate at these elbows much as it did in the elbow above the riser. Both transitions were cleaned out periodically by passing a plumbers snake through the area.

These plugged areas and deposits led to the need to dismantle and clean these areas about once per day. Blockage in the ductwork, and hence the need for maintenance was indicated by a loss of vacuum in the plenum, and or an increase in the vacuum present in the ductwork between the film cooler and the quench. Often this reduction in vacuum was noted during the manual data recording rounds. At times pressure fluctuations in the melter caused short-duration positive pressure excursions, resulting in some fugitive emissions. When these situations occurred, feeding was stopped and the various trouble spots were cleaned.

Several lessons learned have been taken from these results and will be employed in the next melter demonstration, namely:

- Relocation of the melter-offgas outlet and film cooler - The ceramic material buildup, and to some extent the salt accretions downstream, most likely were have been caused by feed entrainment in the offgas. The melter outlet was located approximately 6 inches above the melt surface through the side of the plenum. For the next run, the offgas outlet will be moved to the top of the melter, which will increase the distance between the melt surface and the offgas interface to approximately 20 inches. The film cooler and riser will both be in a vertical orientation, which will encourage any fallout in this section to drop back into the melter, rather than rest on the ductwork and contribute to the deposits.

- Alteration of the offgas piping to minimize elbows – In addition to relocating the melter outlet to the top of the plenum, the elbows described above will be changed to sweep elbows, and the two adjacent elbows will be removed, as well as minimized changes in pipe inner diameter.

- Replacement of film cooler –Proper film cooler designs (as used in DWPF and WVDP) are 'bayonette' style, in which the quench function begins immediately as the offgas passes into the film cooler at or around the hot face of the plenum. The new film cooler and new offgas exit location are expected to create even more favorable conditions downstream, allowing less material accretion.

5. MELTER PRODUCT CHARACTERIZATION

5.1 Glass Viscosity

Molten glass viscosity is dependent on temperature and composition. Glass viscosity influences cold cap formation, and inversely affects volatilization from the melt. Glass viscosity is also inversely proportional to melt reactivity, melt corrosion, devitrification rate on cooling, and pouring properties. . Glass viscosity can also influence the rate of primary phase crystallization at the liquidus temperature (T_L) and can influence the glass annealing properties once poured into a glass cannister[13].

Through the DWPF operating experience, a glass viscosity range of between 20 and 100 Poise (2-10 pascal-seconds) has been recommended for joule heated, refractory lined glass melters operating at 1150°C. Maintaining the glass viscosity within this range minimizes processing problems (pouring, corrosion) associated with viscosity. Thus, it is necessary to characterize the viscosity as it relates to melt temperature before processing in a full-scale melter.

Two samples were analyzed to determine the glass viscosity (η) as a function of temperature using a method consistent with ASTM standard procedure C965-95[13]. The two glass samples analyzed were GLAS-183, collected from the final pour stream of the melter, and GLAS-216, taken from the last poured crucible (these glass samples were both drawn from the melter after chemical steady-state was achieved, and, therefore, should be the same compositionally). Table 5.1 shows the target and measured composition values for these samples. Figure 5.1 shows viscosity as a function of temperature for both glasses. The measured η values are presented in Table 5.2 It should be noted that when the measured data were curve fitted to the Fulcher equation:

$$\ln(\text{Pa}\bullet\text{s})\ \eta = A+B/(T-To),$$

a calculated η of 2.68 Pa•s at 1150°C for GLAS-183 matches almost exactly with the 2.54 Pa•s predicted η published in Peeler et al[3] for the same target composition. A calculated η of 3.57 Pa•s resulted for GLAS-213. Both glass sample's are within the targeted η range of 2-10 Pa•s at 1150°C.

Table 5.1. Viscosity glass sample composition target and measured values.

Element	Feed Target	GLAS-183	GLAS-213
Al	4.40%	4.70%	4.69%
B	6.01%	3.06%	2.87%
Ca	2.95%	3.11%	3.14%
Ce	0.00%	0.00%	0.00%
Cs	0.00%	0.01%	0.03%
Cr	0.04%	0.05%	0.05%
Cu	0.01%	0.02%	0.02%
Gd	0.01%	0.01%	0.01%
Fe	5.14%	5.16%	4.69%
Li	1.61%	1.58%	1.73%
Mg	0.07%	0.17%	0.19%
Mo	0.01%	0.18%	0.24%
Ni	0.02%	0.03%	0.04%
P	0.48%	0.13%	0.10%
K	1.88%	2.20%	2.14%
Ru	0.00%	0.00%	0.00%
Si	21.05%	19.00%	18.66%
Na	11.59%	10.40%	10.50%
Sr	0.00%	0.01%	0.01%
S	1.06%	0.29%	0.30%
Zn	0.02%	0.02%	0.02%
Cl	0.26%	0.00%	0.01%
F	0.17%	0.00%	0.00%

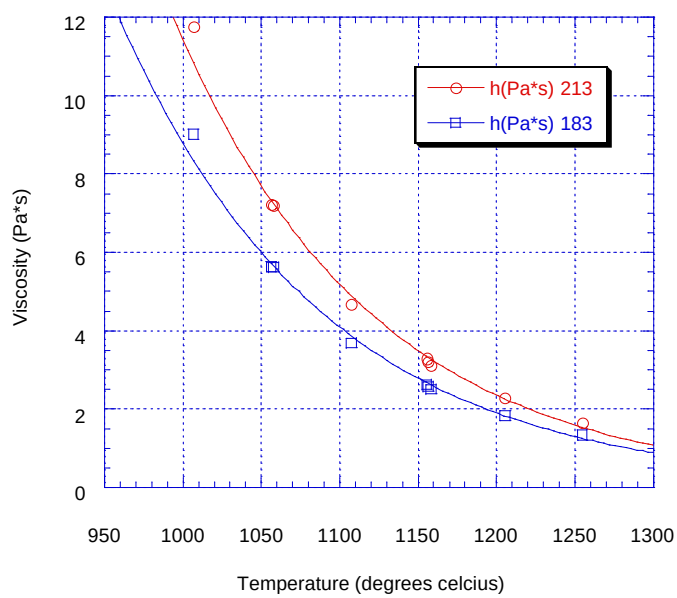

Figure 5.1. Temperature-viscosity profiles for two glass samples.

Table 5.2. Measured viscosity and temperature values.

GLAS-183 h (Pa×s)	GLAS-183 Temperature (C)	GLAS-213 h (Pa×s)	GLAS-213 Temperature (C)
1.35	1254.6	1.65	1254.3
1.84	1205.6	2.28	1205.2
2.57	1156.7	3.21	1156.4
3.69	1107.2	4.67	1106.7
5.64	1057.0	7.22	1056.9
9.02	1006.5	11.75	1006.5

5.2 Glass Durability

Durability of a waste form primarily refers to its ability to resist degradation by aqueous processes. Degradation by these processes over geologic time is the most likely mechanism to result in loss to the environment of the hosted radionuclides and hazardous species. Therefore, a waste form must exceed durability properties in order to qualify for repository storage.

The Product Consistency Test (PCT)[16] was developed to evaluate the durability of homogeneous and devitrified glasses by measuring the concentrations of the chemical species released from a representative crushed glass sample to a test solution under enhanced leaching conditions.

Four melter glasses and the EA reference glass were subject to the PCT Method B leach analysis as described in ASTM C1285-97. Glass samples GLAS-171, GLAS-213, GLAS-216, and GLAS-847 represent the first poured sample after two melter tank volume turnovers, the 13th crucible (one crucible after steady-state was attained, the final poured crucible (after approximately 3.75 melter volume turnovers), and glass mined from the center of the melt tank after cool down. Table 5.3 shows the target and measured composition values for these samples. The PCT was conducted on duplicate samples of each glass including the EA glass and a blank. Normalized releases calculated based on both "target" and "analyzed" glass compositions are presented in Table 5.4 and Table 5.5. All glasses met the conservative upper release limit of 1 g/m^2 and were well below the EA reference glass release values for B, Li, Na, and Si.

Table 5.3. PCT glass sample composition target and measured values.

Element	Feed Target	GLAS-171	GLAS-213	GLAS-216	GLAS-847
Al	4.40%	4.43%	4.69%	4.63%	4.86%
B	6.01%	2.78%	2.87%	3.01%	3.01%
Ca	2.95%	2.81%	3.14%	2.99%	3.17%
Ce	0.00%	0.00%	0.00%	0.00%	0.00%
Cs	0.00%	0.00%	0.03%	0.00%	0.01%
Cr	0.04%	0.05%	0.05%	0.05%	0.06%
Cu	0.01%	0.02%	0.02%	0.02%	0.02%
Gd	0.01%	0.01%	0.01%	0.01%	0.01%
Fe	5.14%	4.72%	4.69%	4.85%	5.23%
Li	1.61%	1.74%	1.73%	1.79%	1.62%
Mg	0.07%	0.14%	0.19%	0.15%	0.19%

Mo	0.01%	0.24%	0.24%	0.19%	0.20%
Ni	0.02%	0.04%	0.04%	0.03%	0.03%
P	0.48%	0.11%	0.10%	0.12%	0.12%
K	1.88%	1.82%	2.14%	1.96%	2.30%
Ru	0.00%	0.00%	0.00%	0.00%	0.00%
Si	21.05%	19.51%	18.66%	18.64%	19.09%
Na	11.59%	10.40%	10.50%	10.80%	10.40%
Sr	0.00%	0.01%	0.01%	0.01%	0.01%
S	1.06%	0.28%	0.30%	0.29%	0.32%
Zn	0.02%	0.02%	0.02%	0.02%	0.02%
Cl	0.26%	0.01%	0.01%	0.01%	0.00%
F	0.17%	0.00%	0.00%	0.00%	0.00%

Table 5.4. Normalized PCT Release Values (based on targeted compositions).

Glass	Log r_B (g/m^2)	Log r_{Li} (g/m^2)	Log r_{Na} (g/m^2)
171	0.66	0.81	0.75
213	0.36	0.46	0.42
216	0.45	0.50	0.47
847	0.52	0.60	0.56
EA Glass	8.85	5.04	6.45
EA Reference Value	8.35	6.67	4.78

Table 5.5. Normalized PCT Release Values (based on analyzed compositions).

Glass	Log r_B (g/m^2)	Log r_{Li} (g/m^2)	Log r_{Na} (g/m^2)
171	0.71	0.69	0.77
213	0.37	0.39	0.43
216	0.45	0.42	0.46
847	0.53	0.57	059
EA Glass	8.43	4.44	5.92
EA-Reference Value	8.35	6.67	4.78

5.3 Liquidus Temperature

The liquidus temperature was determined for sample GLAS-183 using the uniform temperature method as described by Vienna et al. (1998). Liquidus temperature (T_L), is defined as the maximum temperature at which equilibrium exists between a molten glass and its primary crystalline phase[16]. If the nominal melt temperature is below $T_{L,}$ (or cold spots exist within the melter) crystallization may occur and can impact processing. For example, crystals can plug the melter drain tube. Product performance

such as durability can be affected due to preferential leaching of enriched crystalline or vitreous phases that may exist in devitrified product. To avoid the potential negative effects of crystallization within the melter, a T_L criterion of 100°C below the nominal melt temperature (T_M) is adopted (i.e., $T_M > T_L+100^oC$)[17]. The 100°C differential provides an adequate buffer to avoid crystallization while considering variations or uncertainties in melter temperature, composition and T_L measurement.

The T_L for GLAS-183 was determined to be 921 °C. A phase of minute particles dispersed throughout the glass was visible using optical microscopy at 50X to 200X. A sample with the highest concentration of particles was analyzed by SEM and XRD but the particulate phase was below the detection limit for XRD and attempts to identify it with the SEM were also unsuccessful.

An additional test was completed to assess the remelting of secondary phases formed at a temperature below T_L. Two glass samples (GLAS-183 and GLAS-213) were heat treated at 800°C for 63 hours to maximize the formation of crystalline phase. . Again, as with the GLAS-183 T_L measurement, minute particles were visible using optical microscopy but were not detectable via SEM and XRD. Both samples were then remelted at 1150 °C for 4 hours, air quenched and analyzed via optical microscopy, SEM, and XRD for the presence of secondary phases. No secondary phases were detected after remelting, providing an indication that devitrification within a drain tube (EV-16 did not have a drain tube, but this statement is in consideration of the production melter) is not likely to impede pouring once initiated.

5.4 Phase Separation

A few glass samples collected from the melter pour stream and collection crucible had a secondary phase, unlike the secondary phase of particles from the liquidus testing, in the form of a "nodule" or a "streak". SEM analysis performed on one of the nodules showed a high concentration of molybdenum, most likely originating from corrosion and erosion of the molybdenum electrodes and drain orifice. This formation is not considered a problem since a production Joule-heated melter for the vitrification of SBW would likely use Inconel 690 electrodes. The SEM data for GLAS-208A is presented in Figure 5.2.

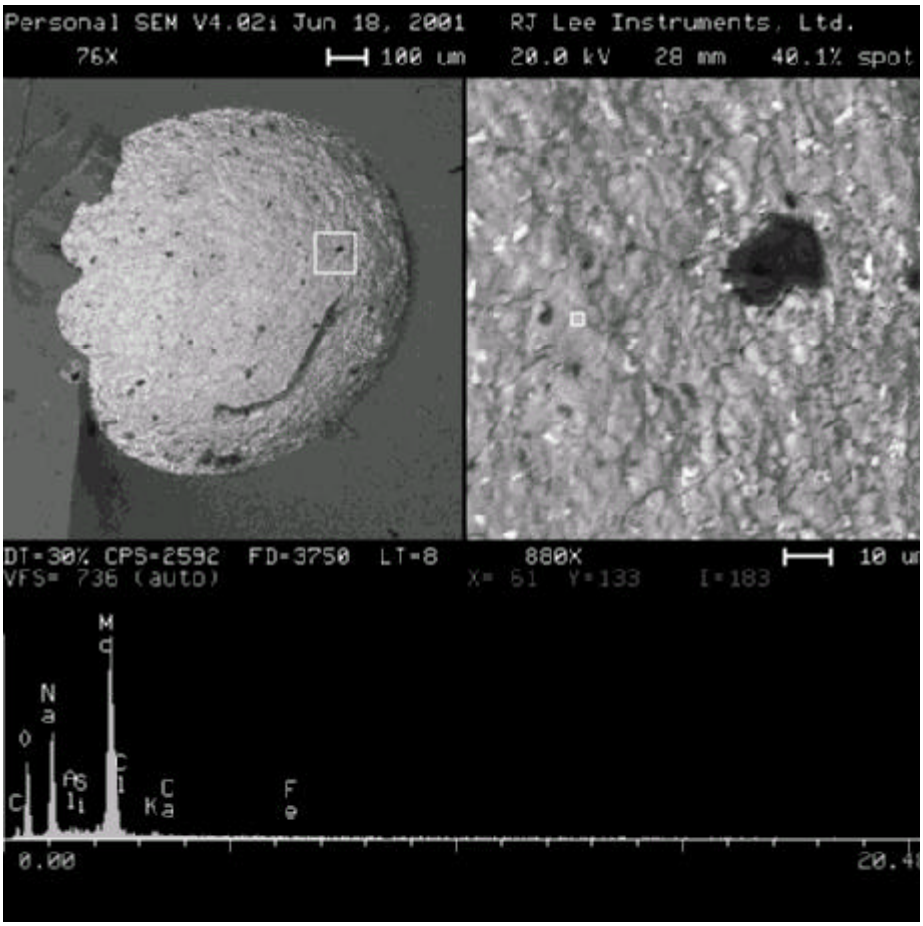

Figure 5.2. Secondary electron (or backscatter electron) micrograph and energy dispersive spectrum photo of a molybdenum nodule.

5.5 Redox Results

As stated, the redox ratio (Fe^{2+}/Fe_{total}) remained below the targeted value of 0.2 to 0.3, as shown in Figure 5.3. These values show an approximate, steady-state average of 0.14. Several of these same samples were then analyzed at PNNL. PNNL data, in Table 5.6, show lower ratios than INEEL measurements, indicating even more oxidized glass. This explains the amount of oxidation shown on the molybdenum electrodes and drain. For comparison, the INEEL redox method is presented in Appendix H.

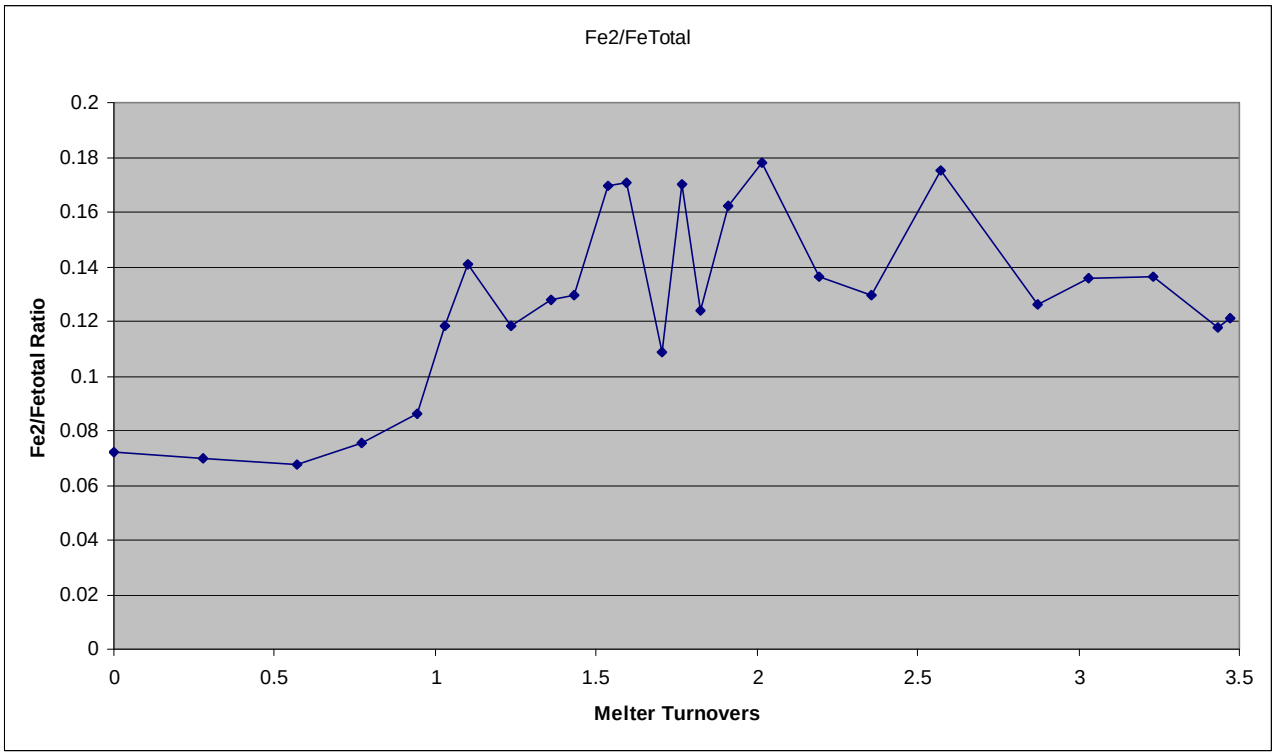

Figure 5.3. Redox ratio (INEEL method) of glass versus melter turnovers.

Table 5.6. PNNL redox measurements and comparison to INEEL measurement of same samples.

Sample ID	Mass	Absorbance				Mass (mg)			Fe_{tot}	Fe II/Fe III	Fe II/Fe_{tot}	INEEL Measured Values	Difference
	(g)	Fe II	Fe II diln	Fe_{tot}	Fe_{tot} diln	Fe II	Fe_{tot}	Fe III	(wt%)				
A	0.0371	0.350	1	0.376	10	0.156	1.67	1.52	4.51	0.103	0.093	0.121	30%
A dup	0.0323	0.298	1	0.318	10	0.133	1.41	1.28	4.38	0.103	0.094	0.121	29%
B	0.0289	0.287	1	0.288	10	0.128	1.28	1.15	4.43	0.111	0.100	0.1176	18%
B dup	0.0320	0.310	1	0.307	10	0.138	1.37	1.23	4.27	0.112	0.101	0.1176	16%
C	0.0356	0.449	1	0.355	10	0.200	1.58	1.38	4.44	0.145	0.127	0.1843	46%
C dup	0.0326	0.384	1	0.324	10	0.171	1.44	1.27	4.42	0.135	0.119	0.1722	45%
D	0.0294	0.341	1	0.302	10	0.152	1.34	1.19	4.57	0.127	0.113	0.12	6%
D dup	0.0384	0.435	1	0.387	10	0.194	1.72	1.53	4.49	0.127	0.112	0.1283	14%
E	0.0349	0.647	1	0.090	10	0.288	0.397	0.109	1.14	2.65	0.726	0.74[1]	2%
E dup	0.0316	0.596	1	0.081	10	0.266	0.357	0.091	1.13	2.91	0.744	0.74	-1%
NIST std	0.0312	0.591	1	0.332	2.5	0.263	0.369	0.106	1.18	2.48	0.713	0.74	4%
NIST std dup	0.0301	0.517	1	0.295	2.5	0.230	0.328	0.098	1.09	2.36	0.702	0.74	5%

1 - 0.74 is the standard measurement of the NIST obsidian rock, not the INEEL measured value.

5.6 Secondary Waste Characterization

5.6.1 Solids Condensed in Offgas Lines

Solid material collected in the offgas piping between the melter and the quench column. On two occasions, build-up of solids in the duct between the melter and the film cooler obstructed flow. The film cooler and adjacent ducting was dismantled and cleaned. As this work was done, samples of thedeposits at the film cooler, as well as on piping upstream and downstream of the film cooler were taken. The compositions of these samples are shown in Table 5.7. Table 5.8 provides additional information from X-ray Diffraction (XRD) analysis of the solids.

Table 5.7. Offgas condensed solids composition.

Element	OFGS-817 (upstream from film cooler)	OFGS-809(from film cooler)	OFGS-811 (downstream from film cooler)	OFGS-816 (from offgas line horizontal section downstream from film cooler)
	(mass%)	(mass%)	(mass%)	(mass%)
Al	3.79	0.69	0.33	0.65
B	4.47	3.22	3.33	3.09
Ca	3.15	1.14	1.07	0.92
Ce	0.00	0.00	0.00	0.00
Cs	0.11	0.16	0.16	0.14
Cr	0.11	0.46	0.11	0.08
Cu	0.02	0.02	0.02	0.02
Gd	0.01	0.00	0.00	0.00
Fe	2.34	1.40	0.25	0.17
Li	1.92	1.44	1.58	1.47
Mg	0.15	0.04	0.03	0.02
Mo	0.33	1.33	1.93	0.71
Ni	0.03	0.29	0.01	0.02
P	0.14	0.12	0.07	0.08
K	6.06	8.31	8.92	8.37
Ru	0.00	0.00	0.00	0.00
Si	3.12	0.39	0.12	0.46
Na	20.60	23.50	23.40	22.70
Sr	0.01	0.00	0.00	0.00
S	2.41	2.99	2.14	1.81
Zn	0.02	0.01	0.00	0.00
Cl	0.02	0.04	0.04	0.04
F	0.01	0.02	0.02	0.01
NO3	0.03	0.09	0.10	0.15

PO4	0.00	0.00	0.00	0.00
SO4	0.06	0.08	0.05	0.04
Total	48.91	45.74	43.68	40.95

Table 5.7 validates high entrainment of feed.

Table 5.8. XRD results for condensed solids.

Sample	XRD Results
Offgas 817 (upstream from film cooler)	KCl (Sylvite)and $Na_8[AlSiO_4]_6(NO_2)_2$ are major crystalline components of this sample. . The other components could not be determined with certainty. . The following compounds are possibly present: $KLiSO_4$, $LiAlSi_4O_{10}$, $LiFeMoO_4Cl$, $K_{0.2}Na_{0.8}Cl$ (Halite), CaZrO3, Fe2SiO4 (Fayalite), Ca3Al2O6, Na2Ca(PO4)F (Nacaphite), Ca4Si2O7F2 (Cuspidine) and Fe9S10.
Offgas 809 (from film cooler)	KCl (Sylvite) and KNO3 (Niter) are major crystalline components of this sample. The other crystalline components could not be determined with certainty. . The following compounds are possibly present: Ca3Al2O6, (Na,Ca)Al(Si,Al)3O8 (Albite, calcian, ordered), Na3FSO4 (Kogarkoite), Fe2Fe(BO3)O2 (Vonsenite), NaBO2, SrSiO3, Mg2P4O12, Al2(SO4)3 (Millosevichite) and Na2CaAl4Si4O16 (Lisetite).
Offgas 811 (downstream from film cooler)	KCl (Sylvite) and KNO3 (Niter), appear to be present in this sample. The other crystalline components could not be determined with certainty. . The following compounds are possibly present: SiCl4, Na3MoO4Cl, Ca-Fe-Al-S-Si-O, NaB3O5.2H2O (Ameghinite), Fe2Fe(BO3)O2 (Vonsenite), K2Mn2(SO4)3 (Manganolangbeinite), Na2MoO4, Ca4Al6O12SO4 (Yeelimite), Ca4O(PO4)2/4CaO-P2O5 K0.8Na0.7Ca0.7Al2.8Si5.1O16-6.4H2O (Phillipsite), Li2B2O4/Li2O-B2O3, Na2CaAl4Si4O16 (Lisetite).
Offgas 816 (from offgas line horizontal section downstream from film cooler)	KCl (Sylvite) and KNO3 (Niter) are major crystalline components detected in this sample. The other components could not be determined with certainty. . The following compounds are possibly present: SiCl4, NaAlSiO4, KLi(Al,Li)2(Si3Al)O10m^2 (Lepidolite), CaSO3, NaAlSiO4 (Nepheline), Ca3Fe2(SiO4)3 (Andradite) and LiAlMo2O8/LiAl(MoO4)2.

From these results, it is clear that alkali salts and oxides are the predominant species in the material collected from accretions in the offgas ducting. Salts of alkaline earth and transition metals are present in much lower concentrations. The material found in the duct between the melter and the film cooler had a glassy luster. The composition of this material includes more aluminum, iron, boron, and silicon than the condensed material in the film cooler. This material contained, at least in part, particles of material that is less volatile that were physically entrained from the melter rather than volatilized from the melter. Although the XRD information indicates that KCl and KNO3 are the predominant crystalline species, the anion data imply there is not enough chloride and nitrate to combine with all of the potassium in the material. Further work will need to be done to determine the specific compounds that make up the material coating the off-gas piping.

The total mass of solids collected from the film cooler and piping was not determined. There was enough to clog the film cooler, requiring disassembly and cleaning of the equipment twice during the 8 day melter run.

5.6.2 Solids Filtered from Scrub Solutions

In contrast to the "sticky" solids that collected near the melter outlet, the off-gas particulate matter captured in the wet scrubbers is largely composed of salts and oxides of calcium, aluminum, iron, and silicon. Wet chemical analysis and XRD results are shown in Tables 5.9 and 5.10, respectively, for three filterable solids samples.

Table 5.9. Composition of filterable offgas solids.

Element	Average Feed Composition	FILTR-184 (scrub solution filter)	FILTR-185 (scrub solution filter)	FILTR-186 (scrub solution filter)
		(mass%)	(mass%)	(mass%)
Al		2.61	3.41	3.98
B		0.16	0.25	0.23
Ca		7.14	12.88	15.48
Ce		0.00	0.01	0.00
Cs		0.02	0.03	0.02
Cr		0.31	0.51	1.14
Cu		0.36	0.37	0.31
Gd		0.01	0.01	0.01
Fe		3.29	4.11	6.42
Li		0.60	0.26	0.28
Mg		0.10	0.17	0.13
Mo		0.08	0.18	0.20
Ni		0.39	0.22	0.51
P		1.01	1.32	0.63
K		0.89	9.66	9.37
Ru		0.06	0.10	0.02
Si		18.99	5.13	3.33
Na		1.13	4.24	4.10
Sr		0.05	0.04	0.05
S		0.15	0.42	0.42
Zn		0.95	0.40	0.29
Cl		0.01	0.01	0.00
F		0.06	0.20	0.23
NO3		0.00	0.01	0.01
PO4		0.01	0.00	0.01

SO4	0.01	0.01	0.01
Total	38.39	43.95	47.18

Table 5.10. XRD results for offgas filterable solids.

Sample	XRD Results
Filter 184 (scrub solution filter)	SiO2 (Quartz) is the major crystalline component of this sample. ZrO2 (Baddeleyite) and CaF2 (Fluorite) are minor components, CaMn14SiO24 (Braunite-2Q) and Li2Na4Ca2Al6Si6O24(CrO4)2 are possibly present as minor components.
Filter 185 (scrub solution filter)	SiO2 (Quartz) and K2NaAlF6 (Elpasolite) are the major crystalline components of this sample. . CaF2 (Fluorite) is present as a minor component, Na8(AlSiO4)6(B(OH)4)2 and LiFe(PO4) are possibly present as minors.
Filter 186 (scrub solution filter)	SiO2 (Quartz), CaF2 (Fluorite) and K2NaAlF6 (Elpasolite) are the major crystalline components of this sample. . Cs2KCrF6 and Na7Zr6F31 are possibly present as minors.

A total of 865 grams of filterable solids were collected from the scrub solution during the run. This represents about 0.1 mass % of the total dissolved and undissolved solids fed to the melter.

5.6.3 Salt Layer on Melter Surface

At the end of the test, the contents of the melter were mined out. A salt layer was observed on the top of the cooled glass. The salt had migrated to the cooler areas of the melt during cooling, i.e. the refractory-melt interface area, and may have flowed to that region as the meniscus of the glass melt became more prominent. This material was collected for analysis. The mass of the salt layer was 525 grams. The composition is given in Table 5.11 below.

Table 5.11. Chemical composition of salt layer mined off melter surface.

Element	mass%
Al	0.001
B	0.228
Ca	0.391
Ce	0.000
Cs	0.104
Cr	0.034
Cu	0.003
Gd	0.000
Fe	0.002
Li	1.325
Mg	0.000
Mo	5.756
Ni	0.000
P	0.177
K	5.652
Ru	0.000
Si	0.054
Na	19.769
Sr	0.002
Zn	0.000
Cl	0.729
F	0.143
NO3	0.000
PO4	0.050
SO4	47.726

From these results this material is predominantly composed of sulfate salts. However, the total mass of sulfate ion in this material is only about 242 grams. Based on data from the batch sheet, this amount represents only 3% of the high-sulfate (based on analytical, sulfur content was 26% higher than target) fed to the melter during the run. The phenomenon of molten salt accumulation will need to be carefully monitored in future melter tests.

5.7 Offgas Characterization

The offgas composition was characterized using both continuous emissions monitoring (CEM) and manual sample train collection and analysis. Results of the process monitors used to measure the temperature, pressure, and flowrate of the offgas, the film cooler air, and the scrub solution atomizing air are summarized in this section. The CEM and manual measurement results are summarized in this

section and provided in detail in the Entropy report (provided in Appendix F) and appendices to the Entropy report.

5.7.1 Offgas Flowrate and Composition

The offgas flowrate and composition measurements are summarized in Tables 5.12 through 5.17. Offgas flowrate and composition measurements were made at specific time periods during the test. Measurements are reported for certain time periods that represent initial system startup and diagnostic periods and the specific time periods during which manual sampling was performed. Average values were determined and reported for each of the manual sample train periods and for the average of all of the manual sample train periods, excluding data reported for initial, diagnostic periods.

Table 5.12. Melter outlet offgas flowrates and temperatures.

Date	Time	Activity	In-melt T, C	Plenum T, C	Plenum Outlet T, C	Melter outlet flowrates, scfm (@ 68 F, 1 atm): H2O from feed (a)	H2O from dilu-tion air (b)	H2O from sugar oxida-tion (c)	Total C (d)	Total NOx (d)	Total S as SO2 or SO3 (d)	Total Cl as HCl (d)	Total flowrate from the feed (e)	Total from M/E balance (f)	Total from mass balance (g)	Melter outlet flowrate RPD, % (h)	Air in-leakage (i)
Target ranges			1,150	---	600	---	---	---	---	---	---	---	---	---	---	---	---
4-Apr-01	1007	Initial data check - no feed	1,253	968	600	0.0	0.58	0.0	0.0	0.0	0.000	0.000	0.0	38.5	---	---	---
5-Apr-01	1500-1535	Pitot traverses 1 & 2	1,059	721	570	6.9	0.56	0.87	1.0	0.80	0.022	0.020	9.6	25.4	39.1	43	29.5
6-Apr-01	1303-1318	Pitot traverse 3	1,176	751	557	7.8	0.56	1.0	1.1	0.90	0.025	0.022	10.8	30.4	40.2	28	29.4
7-Apr-01	1715	Low plenum T, low film cooler	1,091	640	453	5.7	NM	0.72	0.78	0.66	0.018	0.016	7.8	17.2	---	---	---
8-Apr-01	0100	Low plenum T, low feedrate	1,216	620	446	5.7	NM	0.72	0.79	0.67	0.018	0.016	7.9	19.2	---	---	---
8-Apr-01	0600	High plenum T, high feedrate	1,160	800	650	10.7	NM	1.4	1.5	1.2	0.034	0.031	14.8	27.7	---	---	---
9-Apr-01	0938-1124	0050-1 sample train	1,135	757	622	10.5	0.34	1.3	1.4	1.2	0.033	0.030	14.5	30.3	32.4	7	17.8
9-Apr-01	1018-1118	TO14-1	1,129	752	615	9.3	0.34	1.2	1.3	1.1	0.029	0.026	12.9	28.3	33.4	16	20.5
9-Apr-01	1208-1319	0060-1 sample train	1,103	779	665	10.0	0.18	1.3	1.4	1.2	0.031	0.028	13.8	17.2	26.1	41	12.3
10-Apr-01	0850-1029	0050-2 sample train	1,073	765	643	8.8	0.28	1.1	1.2	1.0	0.028	0.025	12.2	27.8	32.4	15	20.2
10-Apr-01	1056-1156	TO-14-2	1,049	745	640	10.5	0.28	1.3	1.5	1.2	0.033	0.030	14.6	27.5	32.0	15	17.4
10-Apr-01	1103-1203	0060-2 sample train	1,071	742	629	10.5	0.28	1.3	1.5	1.2	0.033	0.030	14.6	28.9	32.0	10	17.4
10-Apr-01	1235-1335	TO-14-3	1,096	739	634	10.4	0.28	1.3	1.4	1.2	0.033	0.030	14.4	17.0	33.4	65	19.0
10-Apr-01	1232-1332	0050-3 sample train	1,096	739	634	10.4	0.28	1.3	1.4	1.2	0.033	0.030	14.4	17.0	33.4	65	19.0
10-Apr-01	1353-1453	0060-3 sample train	1,088	748	648	9.4	0.28	1.2	1.3	1.1	0.030	0.027	13.0	23.9	28.7	18	15.7
Averages for CEMS/FTIR/manual train periods			1,093	752	637	10.0	0.28	1.3	1.4	1.16	0.031	0.029	13.8	24.2	31.5	28	17.7

a. Calculated assuming all H2O in the feed evolves as H2O in the offgas.
b. Calculated based on %H2O in ambient air = 2.37 % at 80% humidity, typical for the conditions in South Carolina at the time of the test.
c. Calculated based on stoichiometric conversion of H in the sugar to H2O.
d. Calculated from amounts of these constituents in the feed.
e. Sum of the H2O, C, NOx, SOx, and HCl flowrates.
f. The M/E balance uses the film cooler flowrate and temperature, and the melter outlet temperature, to calculate the melter outlet flowrate.
g. The mass balance subtracts the film cooler input air flowrate from the film cooler outlet flowrate to determine the melter outlet flowate.
h. RPD = relative % difference between 2 measurements (M1, M2) of the same parameter = 2 x (M2 - M1) / (M2 + M1) x 100%.
i. Calculated by subtracting the total flowrate of gas evolution from the feed from the melter outlet flowrate determined from the mass balance.

Table 5.13. Film cooler outlet offgas flowrates and temperatures.

Date	Time	Activity	Total melter outlet flowrate, scfm @ 68 F (a)	Film cooler: Air flowrate, scfm @ 68 F (a)	Film cooler dilution factor	Air temp, C	Outlet T, C (point 7)	Outlet T from Entropy, C	Outlet T RPD, % (b)	Outlet flowrate, scfm (Entropy, a, c)	Offgas velocity from Entropy, f/s	dp from process pitot, in. H2O	Outlet flowrate from process pitot, scfm	flowrate from M/E balance, scfm @70 F (d)	Outlet flowrate RPD, % (b, e)
Target ranges			---	20-25	---	---	<350	---	---	---	---	---	---	---	---
4-Apr-01	1007	Initial data check - no feed	---	24.9	---	26.0	374	---	---	---	4.1	4.1	203	63.4	---
5-Apr-01	1500-1535	Pitot traverses 1 & 2	39.1	24.9	1.6	26.0	300	307	2.3	64.0	43.6	---	---	50.3	-24
6-Apr-01	1303-1318	Pitot traverse 3	40.2	40.8	2.0	36.0	261	271	3.8	81.0	51.8	8.0	---	71.2	-13
7-Apr-01	1715	Low plenum T, low film cooler	---	15.9	---	39.0	243	---	---	---	---	1.8	119	33.2	---
8-Apr-01	0100	Low plenum T, low feedrate	---	22.9	---	29.0	216	---	---	---	---	3.1	152	42.1	---
8-Apr-01	0600	High plenum T, high feedrate	---	23.9	---	28.0	360	---	---	---	---	---	---	51.6	---
9-Apr-01	0938-1124	0050-1 sample train	32.4	23.9	1.74	37.0	358	323	-10.4	56.3	39.4	1.7	132	54.2	-4
9-Apr-01	1000-1124	FTIR during 0050-1	32.4	23.9	1.74					56.3					
9-Apr-01	1018-1118	TO14-1	33.4	22.9	1.69	40.0	350	323	-8.0	56.3	39.4	1.4	119	51.2	-9
9-Apr-01	1208-1319	0060-1 sample train	26.1	23.9	1.92	45.0	292	266	-9.2	50.0	31.7	1.4	115	41.1	-20
9-Apr-01	1208-1319	FTIR during 0060-1	26.1	23.9	1.92					50.0					
10-Apr-01	0850-1029	0050-2 sample train	32.4	22.9	1.71	32.0	363	376	3.6	55.3	42.3	0.8	91	50.7	-9
---	---	FTIR during 0050-2								55.3					
10-Apr-01	1056-1156	TO-14-2	32.0	21.9	1.69	38.0	366	376	2.8	53.9	41.2	0.3	56	49.4	-9
10-Apr-01	1103-1203	0060-2 sample train	32.0	21.9	1.69	42.0	367	379	3.1	53.9	41.3	0.4	65	50.8	-6
10-Apr-01	1103-1203	FTIR during 0060-2	32.0	21.9	1.69					53.9					
10-Apr-01	1235-1335	TO-14-3	33.4	17.9	1.54	45.0	318	330	3.8	51.3	36.4	0.9	94	35.0	-38
10-Apr-01	1232-1332	0050-3 sample train	33.4	17.9	1.54	45.0	318	330	3.8	51.3	36.4	1.9	137	35.0	-38
10-Apr-01	1232-1332	FTIR during 0050-3	33.4	17.9	1.54					51.3					
10-Apr-01	1353-1453	0060-3 sample train	28.7	22.9	1.80	46.5	342	347	1.5	51.6	37.6	1.6	128	46.8	-10
10-Apr-01	1353-1453	FTIR during 0060-3	28.7	22.9	1.80					51.6					
Averages for CEMS/FTIR/manual train periods			31.3	21.8	1.71	41.2	342	339	-1.0	53.2	38.4	1.2	104	46.0	-16

a. Flowrate values for the FTIR sample periods are from the sample period with the same or similar time period.
b. RPD = relative % difference between 2 measurements (M1, M2) of the same parameter = 2 x (M2 - M1) / (M2 + M1) x 100%.
c. Calculation per 40CFR60 Appendix A, Method 2. This measurement for film cooler outlet flowrate is most accurate, although it was not continuously measured or recorded.
d. The M/E balance uses the film cooler flowrate and temp, and temperature for film cooler outlet, to calculate film cooler outlet flowrate.
e. Since the flowrate measurement from the process pitot fluctuated, it was not used in feed mass balance calculations or compared to the flowrates determined by mass/energy balances or the Entropy pitot in RPD calculations.

Table 5.14. Offgas composition at the melter outlet.

			Melter outlet offgas composition, dry basis (except where noted) (a)														
Date	Time	Activity	O2, %	CO2, %	CO, ppm	NO, %	NO2, %	NOx, %	HNO3, ppm	N2O, ppm	N2O4 & N2O5, ppm	Total NOx, %, incl. all NxOy species	SO2 corrected for interference, ppm	HCl, ppm (b)		Cl2, ppm	Total Cl as HCl, ppm
4-Apr-01	1007	Initial data - no feed	---	---	---	---	---	---	---	---	---	---	---	---		---	---
5-Apr-01	1500-1535	Pitot traverses 1 & 2	19.0	2.13	4,420	0.83	0.65	1.49	---	---	---	---	56	---		---	---
6-Apr-01	1303-1318	Pitot traverse 3	---	---	---	0.83	0.73	1.55	---	---	---	---	---	---		---	---
7-Apr-01	1715	Low plenum T, low film cooler	---	---	---	1.21	0.81	2.02	---	---	---	---	109	---		---	---
8-Apr-01	0100	Low plenum T, low feedrate	---	---	---	---	---	---	---	---	---	---	---	---		---	---
8-Apr-01	0600	High plenum T, high feedrate	---	---	---	---	---	---	---	---	---	---	---	---		---	---
9-Apr-01	0938-1124	0050-1 sample train	18.2	3.67	4,421	1.24	0.95	2.17	---	---	---	---	350	0.05		---	< 26.8
9-Apr-01	1000-1124	FTIR during 0050-1	---	4.16	3,335	1.12	1.23	2.42	47.3	828	26	2.61	5	1.22		---	---
9-Apr-01	1018-1118	TO14-1	18.3	3.54	4,217	1.21	0.86	2.07	---	---	---	---	327	---		---	---
9-Apr-01	1208-1319	0060-1 sample train	17.6	3.62	4,105	1.30	0.88	2.18	---	---	---	---	278	---		---	---
9-Apr-01	1208-1319	FTIR during 0060-1	---	4.52	3,837	1.12	1.27	2.47	52.1	912	29	2.68	5	2.68		---	---
10-Apr-01	0850-1029	0050-2 sample train	18.3	4.27	3,925	1.45	1.31	2.76	---	---	---	---	630	0.49	<	12.8	< 26.1
---	---	FTIR during 0050-2	No FTIR data - CEMS not online														
10-Apr-01	1056-1156	TO-14-2	18.3	4.21	4,720	1.52	1.38	2.90	---	---	---	---	675	---		---	---
10-Apr-01	1103-1203	0060-2 sample train	18.0	3.84	4,991	1.43	1.36	2.79	---	---	---	---	650	---		---	---
10-Apr-01	1103-1203	FTIR during 0060-2	---	5.46	3,371	1.11	1.49	2.80	89.3	143	167	2.89	10	4.92		---	---
10-Apr-01	1235-1335	TO-14-3	18.2	3.84	3,844	1.38	1.38	2.77	---	---	---	---	-90	---		---	---
10-Apr-01	1232-1332	0050-3 sample train	18.2	4.32	4,474	1.47	1.58	3.05	---	---	---	---	26	0.12	<	17.7	< 35.5
10-Apr-01	1232-1332	FTIR during 0050-3	---	5.60	3,959	1.01	1.75	2.91	81.5	130	152	3.00	8	4.97		---	---
10-Apr-01	1353-1453	0060-3 sample train	17.7	4.61	4,507	1.59	1.48	3.06	---	---	---	---	-40	---		---	---
10-Apr-01	1353-1453	FTIR during 0060-3	---	6.32	3,321	1.26	1.63	3.02	95.4	153	178	3.12	18	7.00		---	---
Averages for the CEM/manual trains			18.1	3.99	4,356	1.40	1.24	2.64	---	---	---	---	312	0.22	<	15.2	< 29.5
Aveages for the FTIR measurements			---	5.21	3,565	1.12	1.47	2.72	73	433	110	2.86	9	4.16		---	4.16
RPD, % (d)			---	26	-20	-22	17	3	---	---	---	---	---	---		---	---
Values most representative of true concentrations (e)			18.1	4.60	4,356	1.40	1.24	2.64	43	241	65	2.86	312	4.16	<	15.2	4.16

Table 5.15. Offgas composition at the melter outlet continued.

Date	Time	Activity	Melter outlet offgas composition, dry basis (except where noted) (a)																	
			HF, ppm		0	F2, ppm		Total F, ppm		HI, ppm	I2, ppm	Total I, ppm	THC, ppm CH4		H2, %	PM, mg/dscm	H2O (wet %) (c)			
4-Apr-01	1007	Initial data - no feed	---			---		---					---		---		---			
5-Apr-01	1500-1535	Pitot traverses 1 & 2	---			---		---					82		---		12.6			
6-Apr-01	1303-1318	Pitot traverse 3	---			---		---					---		---		---			
7-Apr-01	1715	Low plenum T, low film cooler	---			---		---					182		---		---			
8-Apr-01	0100	Low plenum T, low feedrate	---			---		---					---		---		---			
8-Apr-01	0600	High plenum T, high feedrate	--			--		---					---		--		---			
9-Apr-01	0938-1124	0050-1 sample train		<	0.04	<	13.2	<	26.47	<	0.16	0.96	2.07	85		---	3,927	18.8		
9-Apr-01	1000-1124	FTIR during 0050-1	0.14			---		0.14					52		---	---	18.8			
9-Apr-01	1018-1118	TO14-1				---		---					76	<	0.34	---	18.8			
9-Apr-01	1208-1319	0060-1 sample train				---		---					172		---	---	23.6			
9-Apr-01	1208-1319	FTIR during 0060-1	0.40			---		0.40					87		---	---	---			
10-Apr-01	0850-1029	0050-2 sample train	0.04		<	11.8	<	23.59	<	0.13	2.51	5.15	85		---	2,456	16.7			
---	---	FTIR during 0050-2				---									---	---	16.7			
10-Apr-01	1056-1156	TO-14-2	---			---		---					118	<	0.34	---	21.5			
10-Apr-01	1103-1203	0060-2 sample train	---			---		---					100		---	---	21.5			
10-Apr-01	1103-1203	FTIR during 0060-2	0.00			---		0.00					61		---	---	21.5			
10-Apr-01	1235-1335	TO-14-3						---					154	<	0.29	---	26.3			
10-Apr-01	1232-1332	0050-3 sample train	0.05		<	13.1	<	26.19	<	0.17	2.46	5.09	154		---	7,540	26.3			
10-Apr-01	1232-1332	FTIR during 0050-3	0.00			---		0.00					104		---	---	26.3			
10-Apr-01	1353-1453	0060-3 sample train				---		---					100		---	---	24.2			
10-Apr-01	1353-1453	FTIR during 0060-3	0.00			---		0.00					68		---	---	24.2			
Averages for the CEM/manual trains			0.05		<	12.7	<	25.42	<	0.15	1.98	4.10	116	<	0.32	4,998	21.2			
Aveages for the FTIR measurements			0.11			---		0.11		---	---	---	75		---	---	---			
RPD, % (d)			---			---		---		---	---	---	-44		---	---	---			
Values most representative of true concentrations (e)			0.11		<	12.7		0.11	<	0.15	1.98	4.10	116	<	0.32	4,998	21.3			

ND = Not detected

a. Standard temperature is 68 F and standard pressure is 1 atm.

b. HCl data from the CEM was all less than 0, suggesting uncorrectable interferences in this measurement. This result is consistent with results of NWCF calciner HCl measurements.
c. % moisture from the manual trains is recorded here. For periods when there were no manual sample trains, %H2O was estimated from the amount of H20 in the feed, the feedrate, and the %H2O in the leakage and film cooler air.
d. RPD = relative % difference between 2 measurements (M1, M2) of the same parameter = 2 x (M2 - M1) / (M2 + M1) x 100%.
e. These values are recommended based on evaluation of the CEMS, manual train, and FTIR data. In some cases agreement is good, with RPD less than ±25%. In those cases, the CEM or manual train data is recommended, and the FTIR data corroborates that data. When the measurements for the same parameters are less consistent, then the larger values are usually used to provide more conservatively high emission results. The FTIR THC results are lower than the CEMS THC results because the FTIR THC value is the CH4-equivalent sum of the CH4, C2H4, and C3H8 FTIR measurements. This sum does not include other potential hydrocarbons in the 1-10 ppm range that are included in the CEM THC measurement. For CO2, the average value of the FTIR and CEMS data was used to best approximate the true CO2 level.

Table 5.16. Offgas composition at the film cooler outlet.

			Film cooler offgas composition, dry basis (except where noted) (a)															
Date	Time	Activity	O2, %	CO2, %	CO, ppm	NO, %	NO2, %	NOx, %	HNO3, ppm	N2O, ppm	N2O4 & N2O5, ppm	Total NOx, %, incl. all NxOy species	SO2 correc-ted for interfer-ence, ppm	HCl, ppm (b)		Cl2, ppm		Total Cl as HCl, ppm
4-Apr-01	1007	Initial data - no feed	20.8	0.10	0	0.00	0.00	0.00	---	---	---	---	2	---		---		---
5-Apr-01	1500-1535	Pitot traverses 1 & 2	19.8	1.30	2,700	0.51	0.40	0.91	---	---	---	---	34	---		---		---
6-Apr-01	1303-1318	Pitot traverse 3	---	---	---	0.41	0.36	0.77	---	---	---	---	---	---		---		---
7-Apr-01	1715	Low plenum T, low film cooler	19.6	1.40	3,600	0.60	0.40	1.00	---	---	---	---	54	---		---		---
8-Apr-01	0100	Low plenum T, low feedrate	20.5	1.20	3,500	0.45	0.30	0.75	---	---	---	---	51	---		---		---
8-Apr-01	0600	High plenum T, high feedrate	19.8	2.30	2,800	0.80	0.75	1.55	---	---	---	---	226	---		---		---
9-Apr-01	0938-1124	0050-1 sample train	19.4	2.11	2,543	0.71	0.54	1.25	---	---	---	---	201	0.03	<	7.7	<	15.43
	1000-1124	FTIR during 0050-1	---	2.39	1,918	0.65	0.71	1.39	27	476	15	1.50	3	0.70				0.70
9-Apr-01	1018-1118	TO14-1	19.4	2.10	2,500	0.72	0.51	1.23	---	---	---	---	194	---		---		---
9-Apr-01	1208-1319	0060-1 sample train	19.3	1.89	2,142	0.68	0.46	1.14	---	---	---	---	145	---		---		---
	1208-1319	FTIR during 0060-1	---	2.36	2,002	0.59	0.66	1.29	27	476	15	1.40	3	1.40				1.40
10-Apr-01	0850-1029	0050-2 sample train	19.4	2.50	2,300	0.85	0.77	1.62	---	---	---	---	369	0.29	<	7.5	<	15.29
	---	FTIR during 0050-2	No FTIR data - CEMS not online						---	---	---	---	---	---		---		---
10-Apr-01	1056-1156	TO-14-2	19.4	2.50	2,800	0.90	0.82	1.72	---	---	---	---	401	---		---		---
10-Apr-01	1103-1203	0060-2 sample train	19.2	2.28	2,961	0.85	0.81	1.66	---	---	---	---	385	---		---		---
	1103-1203	FTIR during 0060-2	---	3.24	2,000	0.66	0.89	1.66	53	85	99	1.71	6	2.92				2.92
10-Apr-01	1235-1335	TO-14-3	19.2	2.50	2,500	0.90	0.90	1.80	---	---	---	---	-59	---		---		---
10-Apr-01	1232-1332	0050-3 sample train	19.2	2.81	2,910	0.96	1.03	1.99	---	---	---	---	17	0.08	<	11.5	<	23.08
	1232-1332	FTIR during 0050-3	---	3.64	2,575	0.66	1.14	1.89	53	85	99	1.95	5	3.23				3.23
10-Apr-01	1353-1453	0060-3 sample train	19.2	2.56	2,505	0.88	0.82	1.70	---	---	---	---	-22	---		---		---
	1353-1453	FTIR during 0060-3	---	3.51	1,846	0.70	0.91	1.68	53	85	99	1.74	10	3.89				3.89
Averages for the CEM/manual trains			19.3	2.36	2,573	0.83	0.74	1.57	---	---	---	---	181	0.13	<	8.9	<	17.93
Aveages for the FTIR measurements			---	3.03	2,068	0.65	0.86	1.58	43	241	65	1.66	5	2.43		---		2.43
RPD, % (d)			---	25	-22	-24	15	1	---	---	---	---	---	---		---		---
Values most representative of true concentrations (e)			19.3	2.69	2,573	0.83	0.74	1.57	43	241	65	1.66	181	2.43		8.90		2.43

Table 5.17. Offgas composition at the film cooler outlet continued.

Date	Time	Activity	HF, ppm	F2, ppm	Total F, ppm	HI, ppm	I2, ppm	Total I, ppm	THC, ppm CH4	H2, %	PM, mg/ dscm	H2O (wet %) (c)
4-Apr-01	1007	Initial data - no feed	--	--	---	--	--	---	3	--	--	2.4
5-Apr-01	1500-1535	Pitot traverses 1 & 2	--	--	---	--	--	---	50	--	--	12.6
6-Apr-01	1303-1318	Pitot traverse 3	--	--	---	--	--	---	---	--	--	---
7-Apr-01	1715	Low plenum T, low film cooler	--	--	---	--	--	---	90	--	--	---
8-Apr-01	0100	Low plenum T, low feedrate	--	--	---	--	--	---	100	--	--	---
8-Apr-01	0600	High plenum T, high feedrate	--	--	---	--	--	---	---	--	--	---
9-Apr-01	0938-1124	0050-1 sample train	< 0.02	< 7.60	15.22	< 0.09	0.55	1.19	49	--	2,259	18.8
	1000-1124	FTIR during 0050-1	0.08	0.00	0.08				30	---	---	18.8
9-Apr-01	1018-1118	TO14-1			---				45	< 0.20	---	18.8
9-Apr-01	1208-1319	0060-1 sample train			---				90	---	---	23.6
	1208-1319	FTIR during 0060-1	0.21		0.21				46	---	---	---
10-Apr-01	0850-1029	0050-2 sample train	0.03	< 6.90	13.83	< 0.08	1.47	3.02	50	---	1,439	16.7
	---	FTIR during 0050-2			---				---	---	---	16.7
10-Apr-01	1056-1156	TO-14-2			---				70	< 0.20	---	21.5
10-Apr-01	1103-1203	0060-2 sample train			---				60	---	---	21.5
	1103-1203	FTIR during 0060-2	0.00		0.00				36	---	---	21.5
10-Apr-01	1235-1335	TO-14-3			---				100	< 0.19	---	26.3
10-Apr-01	1232-1332	0050-3 sample train	0.03	< 8.50	< 17.03	< 0.11	1.60	3.31	100	---	4,904	26.3
	1232-1332	FTIR during 0050-3	0.00		0.00				68	---	---	26.3
10-Apr-01	1353-1453	0060-3 sample train			---				56	---	---	24.2
	1353-1453	FTIR during 0060-3	0.00		0.00				38	---	---	24.2
Averages for the CEM/manual trains			0.03	< 7.67	15.36	< 0.09	1.21	2.51	69	< 0.20	2,867	20.0
Aveages for the FTIR measurements			0.06	---	0.06	---	---	---	43	---	---	---
RPD, % (d)			---	---	---	---	---	---	-45	---	---	---
Values most representative of true concentrations (e)			0.06	< 7.67	< 15.39	< 0.09	1.21	2.51	69	< 0.20	2,867	21.3

ND = Not detected

a. Standard temperature is 68 F and standard pressure is 1 atm.

b. HCl data from the CEM was all less than 0, suggesting uncorrectable interferences in this measurement. This result is consistent with results of NWCF calciner HCl measurements.
c. % moisture from the manual trains is recorded here. For periods when there were no manual sample trains, %H2O was estimated from the amount of H20 in the feed, the feedrate, and the %H2O in the leakage and film cooler air.
d. RPD = relative % difference between 2 measurements (M1, M2) of the same parameter = 2 x (M2 - M1) / (M2 + M1) x 100%.
e. These values are recommended based on evaluation of the CEMS, manual train, and FTIR data. In some cases agreement is good, with RPD less than ±25%. In those cases, the CEM or manual train data is recommended, and the FTIR data corroborates that data. When the measurements for the same parameters are less consistent, then the larger values are usually used to provide more conservatively high emission results. The FTIR THC results are lower than the CEMS THC results because the FTIR THC value is the CH4-equivalent sum of the CH4, C2H4, and C3H8 FTIR measurements. This sum does not include other potential hydrocarbons in the 1-10 ppm range that are included in the CEM THC measurement. For CO2, the average value of the FTIR and CEMS data was used to best approximate the true CO2 level.

All offgas measurements (flow, temperature) and samples (CEM, isokinetic) were taken from the riser immediately downstream of the film cooler. These measurements, when adjusted for dilution from the film cooler, represent the emissions from the melter, before the offgas composition is changed in the wet scrubber offgas control system. Melter outlet flowrates (upstream of the film cooler) were calculated using the film cooler outlet measurements with conversions to the conditions at the melter outlet.

5.7.2 Melter Offgas Flow Rate and Conditions

Table 5.12 provides selected summary temperature measurements and calculations of melter offgas flowrates. The amount of offgas resulting from the water evaporation denitration, decomposition/oxidation reactions and volatilization was determined based on the feedrate and composition of the feed. At the average gravimetric feedrate of 0.29 liters/minute, the average offgas flowrate from feed evaporation and volatilization was calculated to be 13.8 scfm (at 20°C and 1 atm). The total melter offgas flowrate was the combined offgas from the feed, plus the flowrate of air inleakage into the melter, and was determined two different ways. The theoretical total melter offgas flowrate conversion of feed to glass was calculated to be 31.5 scfm by subtracting the flowrate of film cooler air from the total offgas flowrate measured at the film cooler outlet. .

For comparison and evaluation of data quality, the melter outlet flowrate was also calculated using a mass and energy balance from the film cooler air flowrate and the film cooler inlet and outlet gas temperatures. This value for the melter outlet flowrate averaged 24.2 scfm. The relative percent difference (RPD) of these two measurements averaged 18%, which is reasonably good agreement considering potential propogated errors. The melter outlet flowrate based on the measured film cooler outlet flowrate and the film cooler air flowrate (31.5 scfm) is considered most accurate, and is used in subsequent calculations, because this calculation is independent of the energy balance, the film cooler inlet and outlet temperature measurements, and the relative specific heats of the melter offgas, the film cooler air, and the film cooler outlet offgas.

Melter air inleakage was determined by difference from the flowrate of offgas from the feed conversion and the total melter offgas flowrate. The melter air inleakage flowrate averaged 17.7 scfm.

5.7.3 Film Cooler Outlet Offgas Flow Rate and Conditions

Table 5.13 summarizes the film cooler outlet offgas flowrate and conditions. The film cooler outlet offgas velocity, measured during specific measurement periods using Entropy's S-type pitot, averaged 53.3 f/s. At this offgas flowrate an average temperature of 339°C, and an average static pressure of about –3 inches H_2O, the offgas velocity averaged 38.4 f/s. This velocity was somewhat lower than the velocity of about 50-60 f/s recommended by Savannah River Site personnel to minimize particulate deposition in that pipe section. While this may have contributed to some of the particulate deposition that occurred during the test series, this was probably not the major cause of the greatest amount of deposition which occurred in the film cooler, in various elbows and horizontal runs downstream of the film cooler, and upstream of the film cooler (where hot, sticky PM was able to adhere to the duct inside walls).

The flowrate measured by Entropy was compared to two other independent determinations of flowrate at this sample location. Melter system process monitoring included a 1/8-inch standard pitot located just downstream of the film cooler outlet location. Offgas flowrate determined from this pitot averaged 104 scfm, nearly twice the flowrate measured by the Entropy probe. The film cooler outlet flowrate was also calculated using a mass/energy balance on the film cooler air flowrate and the air and offgas temperatures. The offgas flowrate determined this way averaged 46.0 scfm. The RPD of this measurement compared to the Entropy measurement was –16%. Of these three measurements of offgas

flowrate, the Entropy measurement, done according to EPA Methods 1A and 2 (40 CFR 60 Appendix A) is considered to be most representative of the true value.

5.7.4 Melter Offgas Composition

While all of the offgas composition measurements were made at the film cooler outlet , the measured concentrations were adjusted for the dilution caused by the film cooler air to estimate the melter outlet concentrations.

The calculated melter outlet concentrations are shown in Tables 5.14 and 5.15. All values except for % H_2O are reported on a dry basis. In some cases, multiple techniques were used to measure the same offgas species. This was done mainly because several different measurement techniques were required to measure all of different gas species. Some of the measurement techniques could detect not only the species targeted by that technique, but also other gas species that were detected by other techniques. For example, the most common measurement technique for NO and NO_2 is continuous monitoring using chemiluminescence. But to measure other N_xO_y species such as N_2O and HNO_3, continuous monitoring using fourier-transform infrared (FTIR) was used. FTIR can also detect NO and NO_2. The added FTIR data for NO and NO_2 corroborates with the chemiluminescence data.

The FTIR and CEM NO_x measurements agreed well. The CEM NO_x measurements averaged 1.40% NO, 1.24% NO_2, and 2.64% NO_x. The FTIR NO measurement averaged –22 relative percent difference (RPD) compared to the CEM NO data, and the FTIR NO_2 data averaged +15 RPD compared to the CEM NO_2 data. These differences are similar to EPA's acceptance criteria of $\pm$20% for relative accuracy of air emissions CEMs used for compliance (40 CFR 60 Appendix B, Performance Specification 2. When these differences are averaged in the total NO_x measurement, the FTIR and CEM data agree within an average of 3 RPD.

Other N_xO_y gas species were detected at measurable levels that were considerably lower than the NO and NO_2 concentrations. These concentrations of these gas species ranged from under 100 ppm to over 200 ppm. Nitrates and nitrites, detected in the Method 0050 samples, were higher at total levels averaging almost 5,000 ppm in the offgas, but these ions in the 0050 sample solutions could have resulted in absorption of some of the NO and NO_2 gases which exist in the offgas at much higher levels.

HCl, was measured using a manual sample train (modified EPA Method 0050). This train also provided Cl_2, total F, and total I measurements. HCl was also measured by FTIR and by an additional CEM (non-dispersive infrared with gas filter correlation (NDIR-GFC)). The use of these multiple HCl measurements for this high NO_x offgas were justified in the end because the NDIR-GFC measurement was not valid due to interference from other species (probably NO_2) in the offgas. The HCl measurements from EPA Method 0050 and from FTIR corroborate each other at very low HCl levels (0-7 ppm). The validity of a single measurement technique, without this corroboration, may have been questioned, because of the low concentrations.

The melter outlet O_2 concentration averaged 18.1% suggesting that only a small portion of O_2 contributed by melter air inleakage was consumed in oxidation reactions with the organic reductant in the feed. The overall plenum gas conditions are still highly oxidative, with relatively high oxygen levels compared to traditional incineration, where efficient oxidation of organic material is achieved at O_2 levels that range around 7-10% (dry). Considerable levels of incompletely oxidized CO (averaging over 4,000 ppm) and total hydrocarbons (averaging over 100 ppm) persist, even with excess O_2 conditions, because of the low average gas temperature 637°C at the melter outlet) compared to traditional incineration at temperatures of 1,000^{o}C or higher. Offgas mixing and residence time in the melter plenum could also be nonrepresentative of traditional incineration conditions and contribute to the observed levels of products

of incomplete oxidation. In future melter designs, higher organics oxidation in the plenum may be possible by optimizing the plenum time, temperature, and mixing conditions.

Even under relatively inefficient organics oxidation conditions, levels of H_2 were not detected at a detection limit of about 0.3%. This detection limit is elevated higher than expected because of NO_2 interference in the H_2 analysis, causing large dilution of the sample. While H_2 levels may exist at concentrations below this detection limit, this result provides some assurance that H_2 levels are more than 10x below the H_2 lower flammability limit (in air) of 4.0%. .

The total flammability of the melter gas based on contributions from H_2, CO, and THC (on a wet basis) is very low. Using flammability limits in air for H_2, CO (12.5%), and ethane (8.25%, conservatively representative of THCs), the total flammability of the melter offgas is less than 9% of the total flammability limit. This estimate does not account for other factors that will affect the actual flammability of the offgas. The O_2 level on a wet basis (only 15% compared to 21% in air) and the higher H_2O level (21.3% compared to typically 1-3% in air) will lower the actual flammability of the gas, but the higher gas temperature will increase the actual flammability of the gas.

SO_2 gas was measured using both a nondispersive ultraviolet (NDUV) CEM and also by FTIR. The high NO_2 levels interfered significantly with the CEM SO_2 measurement. . The amount of NO_2 interference was determined using interference checks for the CEMS, and the amount of interference, based on the measured NO_2 levels, was subtracted from the CEM SO_2 measurements. With this large correction, the CEM SO_2 data (averaging 312 ppm) should be considered an estimate only. The FTIR SO_2 averaged much lower at only 9 ppm. Even though the CEM SO_2 is considered an estimate of the true value, and the FTIR is not considered subject to the same interferences as the CEM SO_2 measurement, the CEM SO_2 values are used in mass balance calculations to provide a more conservatively high estimated of the true SO_2 levels.

5.7.5 Film Cooler Outlet Offgas Composition

Tables 5.16 and 5.17 shows the offgas composition measurements made at the film cooler outlet. The only difference between the concentrations in this table and the melter outlet concentrations is that dilution from the film cooler air is subtracted from these measurements to calculate the melter outlet concentrations. This dilution factor averaged 1.70, based on the film cooler outlet flowrate measured by Entropy and the film cooler air flowrate.

5.7.6 Film Cooler Outlet Particulate Matter and Metals Measurements

Particulate matter (PM) and metals measurements at the film cooler outlet are shown in Tables 5.18 and 5.19.

Table 5.18. Particulate and acid gas (Method 0050) measurements at the film cooler outlet.

	Run 1	Run 2	Run 3	Average
Date	04/09/01	04/10/01	04/10/01	- -
Time	0938-1124	0850-1029	1232-1332	- -
Flow Rate, dscfm @ 68°F, 1 atm	45.7	46.1	37.8	43.2
Flow Rate, dscm	1.294	1.305	1.070	1.223
Moisture Content, % by volume	18.8	16.7	26.3	20.6
Gas Temperature, °F	612	709	626	649
Gas Temperature, °C	322	376	330	343
Particulate, gr/dscf	0.9871	0.6291	2.143	1.253
Particulate, mg/dscm	2259	1439	4904	2867
Particulate, lb/hr	0.387	0.249	0.695	0.444
Hydrogen Chloride, mg/dscm	0.0407	0.0432	0.122	0.0686
Hydrogen Chloride, ppmvd	0.0269	0.0285	0.0805	0.0453
Hydrogen Chloride, lb/hr	6.967E-06	7.457E-06	1.728E-05	1.057E-05
Total Fluorides, mg/dscm	ND	0.0216	0.0271	0.0244
Total Fluorides, ppmvd	ND	0.0260	0.0326	0.0293
Total Fluorides, lb/hr	ND	3.729E-06	3.841E-06	3.785E-06
Chlorine, mg/dscm	ND	1.52	4.78	3.15
Chlorine, ppmvd	ND	0.517	1.62	1.07
Chlorine, lb/hr	ND	2.63E-04	6.78E-04	4.70E-04
Nitrites (as NO2-), gm/dscm	1,026	675	935	879
Nitrites (as NO2-), lb/hr	0.176	0.117	0.132	0.142
Nitrates (as NO3-), gm/dscm	2,572	6,358	10,038	6,323
Nitrates (as NO3-), lb/hr	0.440	1.10	1.42	0.987

"<" indicates that the analyte was not detected at the indicated detection limit for the analysis.

Table 5.19. Metals (Method 0060) measurements at the film cooler outlet.

	Run 1	Run 2	Run 3	Average
Test Date	4/9/01	4/10/01	4/10/01	- -
Run Time	1208-1319	1103-1203	1353-1453	- -
Air Flow Rate, dry scfm @ 68°F, 1 atm	38.19	42.27	39.10	39.85
Air Flow Rate, dry scmm	1.081	1.197	1.107	1.129
Moisture Content, % Volume	23.6	21.5	24.2	23.1
Gas Temperature, ^{o}F	512	713	656	627
Gas Temperature, ^{o}C	266	378	347	330
Aluminum, mg/dscm	< 1.04	0.771	< 0.688	< 0.833
Aluminum, lb/hr	< 1.49E-03	1.22E-03	< 1.01E-03	< 1.24E-03
Boron, mg/dscm	134	97.6	99.9	111
Boron, lb/hr	0.0192	0.0154	0.0146	0.0164
Cadmium, mg/dscm	0.00233	0.00110	0.00226	0.00189
Cadmium, lb/hr	3.33E-06	1.74E-06	3.30E-06	2.79E-06
Calcium, mg/dscm	< 12.0	< 14.1	< 13.5	< 13.2
Calcium, lb/hr	< 0.00172	< 0.00224	< 0.00197	< 0.00198
Cerium, mg/dscm	< 0.0860	< 0.0763	< 0.0894	< 0.0839
Cerium, lb/hr	< 1.23E-04	< 1.21E-04	< 1.31E-04	< 1.25E-04
Cesium, mg/dscm	< 21.4	< 21.4	< 19.2	< 20.7
Cesium, lb/hr	< 0.00306	< 0.00339	< 0.00282	< 0.00309
Chromium, mg/dscm	1.41	1.77	1.54	1.57
Chromium, lb/hr	2.02E-03	2.81E-03	2.25E-03	2.36E-03
Cobalt, mg/dscm	<0.00764	< 0.00930	< 0.00778	< 0.00824
Cobalt, lb/hr	<1.09E-06	< 1.47E-05	< 1.14E-05	< 1.23E-05
Copper, mg/ dscm	< 0.455	< 0.489	0.237	< 0.394
Copper, lb/hr	< 6.51E-04	< 7.75E-04	3.47E-04	< 5.91E-04
Gadolinium, mg/dscm	< 0.0525	< 0.0512	< 0.0535	< 0.0524
Gadolinium, lb/hr	<7.52E-06	< 8.10E-06	< 7.83E-06	< 7.81E-06

	Run 1	Run 2	Run 3	Average
Iron, mg/dscm	2.56	1.30	1.63	1.83
Iron, lb/hr	3.67E-03	2.05E-03	2.39E-03	2.70E-03
Lead, mg/dscm	< 0.00803	0.0114	0.0156	< 0.0116
Lead, lb/hr	< 1.15E-05	1.80E-05	2.28E-05	< 1.74E-05
Lithium, mg/dscm	38.6	39.1	< 37.3	< 38.3
Lithium, lb/hr	0.00552	0.00619	< 0.00547	< 0.00573
Magnesium, mg/dscm	0.436	0.371	0.523	0.443
Magnesium, lb/hr	6.23E-04	5.87E-04	7.67E-04	6.59E-04
Manganese, mg/dscm	0.671	0.709	0.630	0.670
Manganese, lb/hr	9.59E-04	1.12E-03	9.23E-04	1.00E-03
Molybdenum, mg/dscm	< 6.59	< 9.32	< 10.3	< 8.73
Molybdenum, lb/hr	< 0.000943	< 0.00148	< 0.00151	< 0.00131
Nickel, mg/dscm	0.314	0.278	0.283	0.292
Nickel, lb/hr	4.49E-04	4.41E-04	4.14E-04	4.34E-04
Phosphorus, mg/dscm	1.22	1.11	1.11	1.15
Phosphorus, lb/hr	1.74E-03	1.76E-03	1.63E-03	1.71E-03
Potassium, mg/dscm	111	149	111	124
Potassium, lb/hr	0.0159	0.0237	0.0163	0.0186
Ruthenium, mg/dscm	< 0.206	< 0.247	< 0.294	< 0.249
Ruthenium, lb/hr	< 2.95E-04	< 3.92E-04	< 4.30E-04	< 3.72E-04
Sodium, mg/dscm	375	371	336	360
Sodium, lb/hr	0.0536	0.0587	0.0492	0.0538
Strontium, mg/dscm	< 0.0478	< 0.0465	< 0.0525	< 0.0489
Strontium, lb/hr	< 6.83E-05	< 7.37E-05	< 7.69E-05	< 7.30E-05
Zinc, mg/dscm	0.101	0.100	0.264	0.155
Zinc, lb/hr	1.45E-04	1.59E-04	3.87E-04	2.30E-04

"<" indicates that the analyte was not detected at the indicated detection limit for the analysis.

5.7.7 Film Cooler Outlet Volatile Organic Compound Measurements

EPA Method TO-14 was used to measure speciated volatile organic compound (VOC) concentrations in the film cooler outlet offgas. H_2 measurements were also obtained using a different (ASTM) laboratory procedure from the same Summa canister that is used in the TO-14 analysis. These measurements are shown in Table 5.20. The TO-14 samples required a dilution factor of 100:1 to reduce the extremely high levels of NO_x in the samples.

Table 5.20. Film cooler outlet Summa canister measurements.

	Run 1	**Run 2**	**Run 3**	**Average**
Date	04/09/01	04/10/01	04/10/01	- -
Time	1018-1118	1056-1156	1235-1335	- -
Stack parameters are from the M0050 or M0060 run that most closely matches the TO-14 sample time.				
Flow Rate, dscfm @ 68°F, 1 atm	45.69	42.27	37.83	41.93
Flow Rate, dscm	1.294	1.197	1.071	1.187
Moisture Content, % by volume	18.8	21.5	26.3	22.2
Gas Temperature, °F	612	713	626	650
Gas Temperature, °C	322	378	330	344
Hydrogen, % vol	< 0.204	< 0.202	< 0.191	< 0.201
TO-14 Compounds, ppbv				
Acetonitrile	1,792	1,656	1,823	1,757
Isopropyl alcohol	1,931	3,392	3,141	2,821
Methylpentane isomer		2,030	1,853	1,942
Toluene	2,033	1,849	2,286	2,056
Octane	1,947	4,739	4,078	3,588
Unknown C9 hydrocarbon (MW 128)	3,436	6,745	5,857	5,346
Decane			2,971	2,971
Decane / Phenol *	3,055	4,114		3,585
Unknown C11 hydrocarbon (MW 147)	5,080	8,155	7,994	7,076
Unknown C11 hydrocarbon (MW 147)	8,230	12,535	12,099	10,955
Unknown C11 hydrocarbon (MW 147)	2,979	4,689	4,496	4,055
Nitrophenol	23,989	4,284	5,461	11,245
Unknown siloxane	2,247	4,363	5,044	3,885
Dodecane	9,714	12,015	10,517	10,749
Isothiocyanatocyclohexane	3,531	4,636	3,844	4,004
Unknown C13 hydrocarbon (MW 193)	2,369	3,051	2,878	2,766
Unknown C13 hydrocarbon (MW 193)	2,383	3,484	2,417	2,761

5.7.8 Size and Characteristics of Particulate Matter

SEM analysis was performed on bulk PM samples and PM collected on filters from the Method 0050 sample trains. SEM analysis enables visual observation of particle size and characteristics at magnifications up to 40,000x. Table 5.21 shows the results of the SEM analysis.

Table 5.21. PM characteristics.

Sample identification	**Macroscopic appearance**	**Microscopic appearance**	**Figure**
EV16-1 M50-1 Cyclone	Light tan, finely divided powder, some clumps	See discussion in figure captions	5.4,5.5, 5.6
EV16-1 M50-1 Filter	Chalky-white, loose crumbled filter cake		---
EV16-1 M50-2 Filter	Chalky-white, loose crumbled filter cake flakes		---
EV16-1 M50-3 Cyclone	Tan, clumpy powder		5.3
EV16-1 M50-3 Filter	Chalky-white, loose, dusty crumbled filter cake		5.7,5.8

The particle size distribution is based on the three major types of particles – rods, angular particles, and cenospheres. By visual observation, the particle size distribution of these types of particles is estimated in Table 5.22.

Table 5.22. Estimated particle size distribution for EV-16 particulate matter at the film cooler outlet.

	Differential particle size microns					Cumulative particle size distribution	
	Rods (a)	Angular PM	Cenospheres	Total	Weighted total average		
Differential wt % of particle type	25	70	5	100		Particle size, microns	% less than
Particle size, microns							
<0.3	0	10	0	---	7	0.3	7
0.3-1	0	70	10	---	49.5	1	56.5
1-3	0	10	80	---	11	3	67.5
3-10	2	10	10	---	8	10	75.5
10-30	28	0	0	---	7	30	82.5
30-100	70	0	0	---	17.5	100	100
Total	100	100	100	---	100		

a. . The particle size for rods is based on the length, not the diameter.

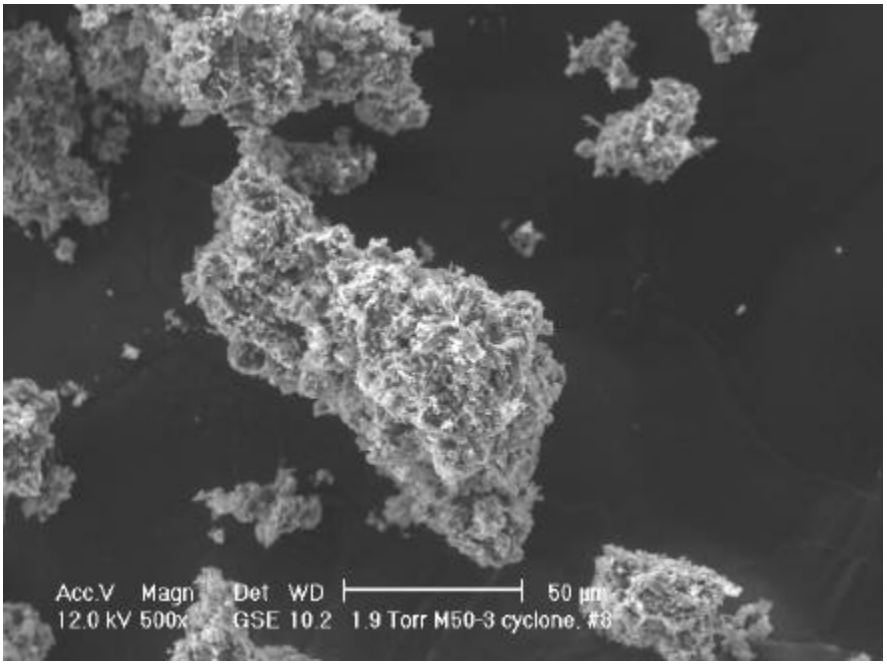

Figure 5.4. Large agglomerated particles of bulk PM captured in a cyclone. These particles range up to 100's of microns in size. The agglomeration is assumed to occur during or after sample collection. Particles as exist in the offgas are not as agglomerated.

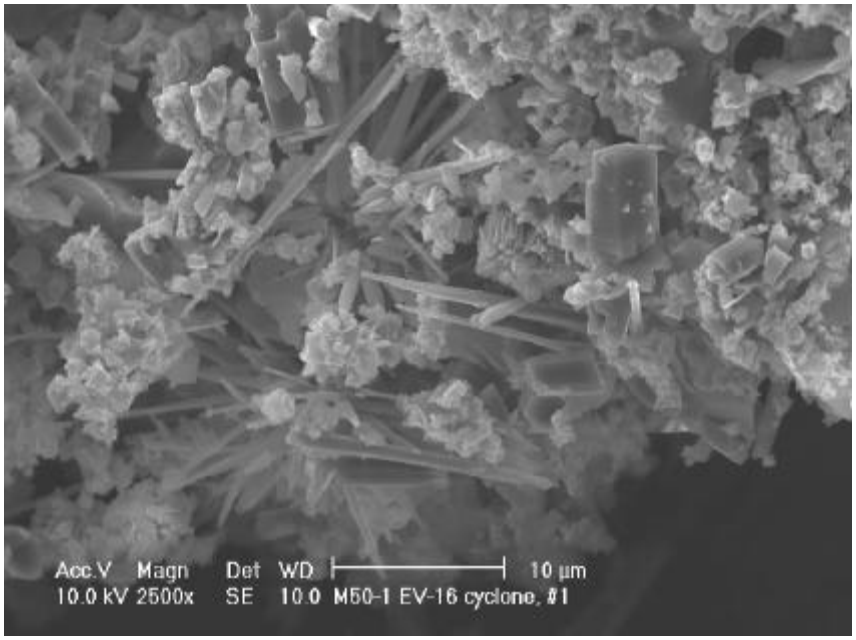

Figure 5.5. Angular particles, rods, and some cenospheres captured in a cyclone. Angular particles range from under 1 micron to over 5 microns in size. Rods are 1 micron or less in diameter and up to 10 or more microns long. These particles are thought to not be agglomerated in the offgas. Angular particles may be feed material entrained in the offgas or may be material that has volatilized in the hot furnace and then condensed material after the film cooler. The long rods are probably material that has volatilized in the hot furnace and then condensed after the film cooler. Small particles adhere to the surfaces of larger particles.

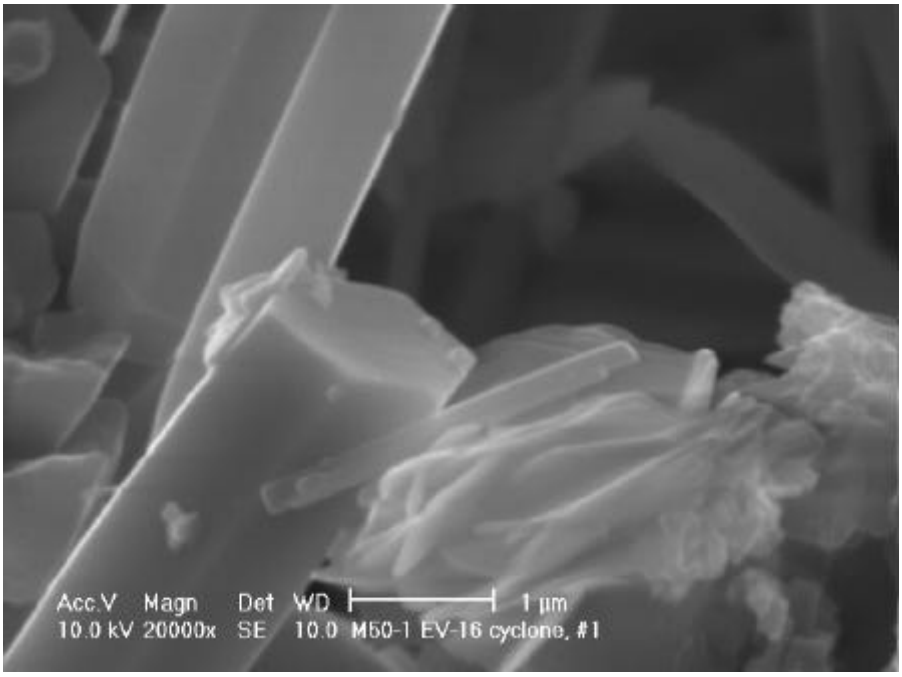

Figure 5.6. Rod of condensed, crystalline PM showing hexagonal crystal structure (captured in a cyclone). This rod is about 1 micron in diameter. A smaller rod, about 0.2 micron in diameter and 2.5 microns long, is nearby.

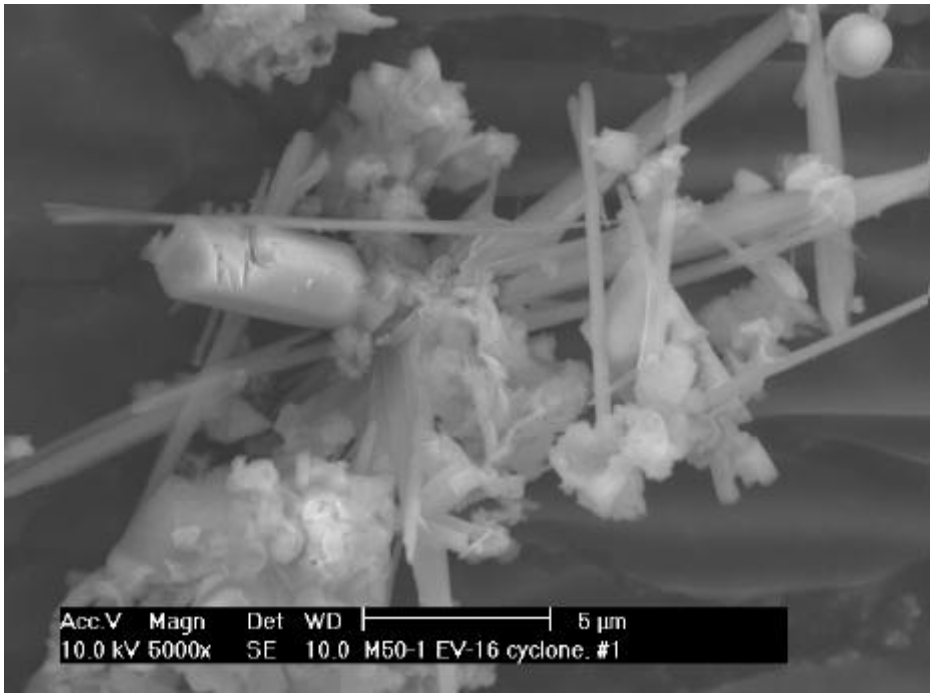

Figure 5.7. This view shows a pentagonal or hexagonal rod, smaller rods, angular particles, and a cenosphere (captured in a cyclone). Cenospheres are feed material entrained into the offgas, softened, expanded from the expansion of internal gases, and then rapidly cooled and frozen after the film cooler.

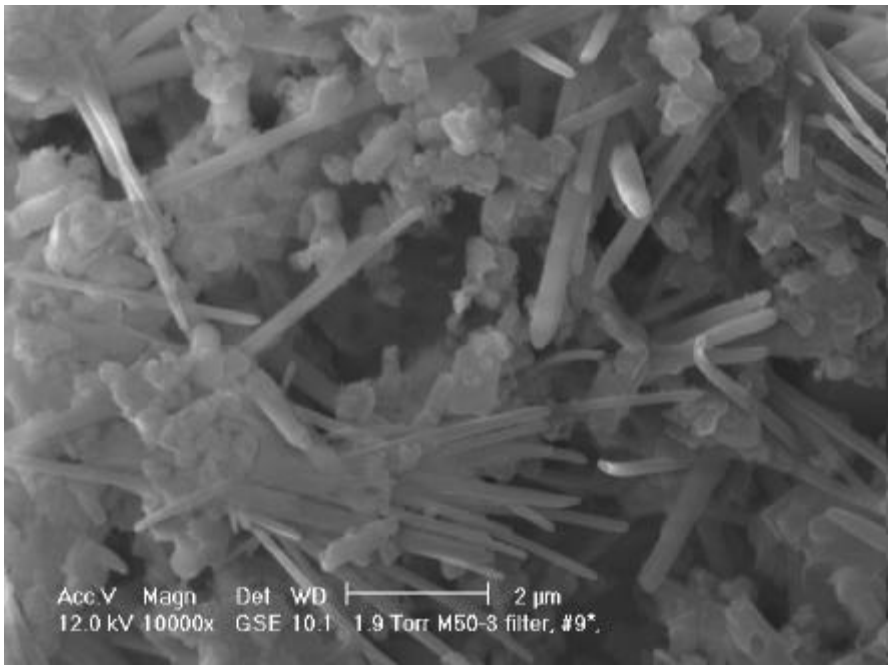

Figure 5.8. PM captured on a filter downstream of the cyclone contains more smaller-diameter rods (~0.3 micron or less in diameter), small ~0.3 micron or less particles, and cenospheres (that are less dense and more easily transported from the cyclone).

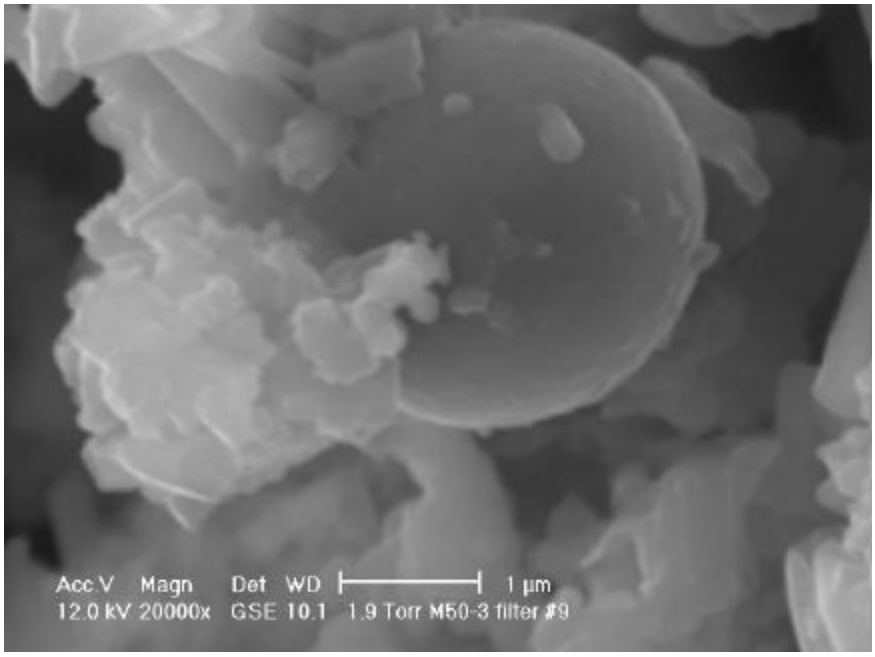

Figure 5.9. A magnified view of a cenosphere and submicron particles captured downstream of the cyclone on a filter suggests some surface layering of condensed material.

6. MATERIAL BALANCE

The primary objective of this demonstration was to gather data necessary to calculate a material balance around the melter operation. This consisted of sampling and analysis of all input and output streams from the process and determining the balances for each element.

6.1 Overall Material Balance

Sampling was conducted under steady state operating conditions to the extent possible in order to provide data reflective of the proposed baseline process. Additional, measurements were taken throughout the test to ascertain the overall material balance around the melter throughout the entire demonstration. Table 6.1 presents the data supporting the overall material balance and the closure value for each element. This analysis uses the feed input, glass output, scrub solution and scrub filtered solids analyses as its basis.

Table 6.1. Overall material balance and closure value for each measured element (Based on ICP and IC analytical results).

	Feed Total		Glass Total		Scrub Solution Total		Filtered Solids Total		Feed - Glass - Solution - Solids		Offgas Measurements[1]		Overall MB Closure	DF	
	moles	**grams**	**moles**	**grams**	**moles**	**grams**	**moles**	**grams**	**moles**	**grams**	**moles**	**grams**	**moles**	Glass	Scrub
Si	4,878	137,005	3,866	108,586	0	10	4	100	1,008	28,309			79%	4.8	1,250
Na	3,078	70,773	2,372	54,540	144	3,302	1	24	561	12,908			82%	4.4	21.3
B	1,742	18,835	1,412	15,270	39	427	0	2	290	3,136			83%	5.3	43.9
Li	1,582	10,979	1,256	8,720	31	213	1	4	294	2,043			81%	4.9	50.7
Al	1,120	30,226	905	24,427	0	1	1	27	214	5,771			81%	5.2	1,100
Fe	555	30,987	489	27,325	0	10	1	35	65	3,617			88%	8.5	691
Ca	499	19,986	397	15,927	1	28	2	91	98	3,941			80%	4.9	168
K	417	16,289	286	11,187	54	2,129	1	47	75	2,926			82%	3.2	7.5
S	94	2,998	47	1,521	10	327	0	3	36	1,148	23	749.60	87%	2.0	9.1
Mg	48	1,164	46	1,114	0	6	0	1	2	43			96%	23.3	176
P	26	796	20	621	0	1	0	9	5	165			79%	4.5	77.1
Cr	6	336	6	296	0	8	0	4	1	29			91%	8.3	28.3
Ni	3	147	6	327	0	2	0	3	(3)	(184)			225%		32.3
Cs	2	296	1	95	0	60	0	0	1	141			52%	1.5	4.9
Zn	2	109	2	111	0	2	0	6	(0)	(9)			108%		14.9
Cu	1	79	3	184	0	2	0	3	(2)	(110)			239%		16.5
Sr	0	31	1	59	0	0	0	0	(0)	(28)			191%		46.9
Mo	0	31	14	1,309	1	70	0	1	(14)	(1,350)			4474%		0.4
Gd	0	48	0	41	0	0	0	0	0	7			86%	7.1	556
Ru	0	26	0	10	0	1	0	1	0	14			45%	1.7	21.1
Ce	0	22	0	16	0	0	0	0	0	6			73%	3.6	238
Cl	51	1,814	66	2,343	18	643	0	0	(33)	(1,172)			165%		2.8
F	10	197	45	852	3	51	0	1	(37)	(707)			459%		3.8
NO3	3,958	245,407	-	-	40	2,484	0	0	3,918	242,923	2,375	147,244	61%		
C	10,206	122,580									8,675	104,193	85%		
H_2O	83,429	1,503,000			16,595	300,797			66,732	1,202,203	90,104	1,623,240	128%		
Total[2]		**465,756**		**274,881**		**7,290**		**361**		**60,644**		**104,943**	**83%**		

1 - Only online offgas measurements dominate scrub solution values are those values are included

2 - Total not counting nitrate and water, which are skewed by reactions not measured

The DFs were calculated based on two different bases, called glass and scrub. The glass DF was calculated by taking the following equation:

Glass DF = 1 / (Material Not In Glass / Material Fed to Melter).

This DF calculation takes into account the uncertainty based on the material balance closure. That is to say that if the material balance closure factor is 85%, the 15% not accounted for is assumed to not be in the glass. Therefore, these DFs are lower than expected. Conversely, the scrub DF is the melter DF calculated be taking into account the material that *was* found in the scrub, or using the equation

Scrub DF = 1 / (Material in Scrub Solution and Filtered Solids / Material Fed to Melter).

This assumes that the material not accounted for *was* retained in the glass, and therefore these DFs are higher. The actual DF is somewhere in between these values, and so these values are presented to bound the DFs based on the data gathered. The same method of calculation is used for the steady-state results.

6.2 Steady-State Material Balance

The chemical conversion of the EV-16 melter has been shown[21] to correspond reasonably well with CSTR theory with complete conversion (95-99%) occurring after three melter volumes[22]. Given that, measurements of interest were made with greater frequency after the melter achieved three turnovers of its volume. Data collected under chemical steady state conditions were used as the basis for the material balance. Table 6.3 presents these data and their associated material balance closure values.

6.3 Isokinetic Sample Train Material Balance

During the steady state portion of the demonstration, three isokinetic offgas samples were taken. There were 3 samples taken, each covering 1 to 1.25 hours of steady-state operation. In all, these samples provide a snapshot of 3.5 hours of the steady-state portion of the demonstration (Note that the overall steady-state portion of the run lasted approximately 48 hours). In addition to the isokinetic samples, offgas scrub solution and solution filter samples were analyzed for comparison. Table 6.4 provides a material balance that is the summation of the three sampling periods. The basis for this balance, as opposed to the overall balance and steady-state balance, are feed in, glass out, and offgas out of the melter. The offgas stream covers the same material that would be gathered in the scrub solution and scrub filtered solids analysis.

Table 6.2. Steady-state material balance and closure value for each measured element.

	Feed Total		Glass Total		Scrub Solution Total		Filtered Solids Total		Feed - Glass - Solution - Solids		Offgas Measurements		Overall MB Closure	DF	
	moles	**grams**	**moles**	**grams**	**moles**	**grams**	**moles**	**grams**	**moles**	**grams**				**Glass**	**Offgas**
Si	2153	60465	1728	48528	0	5	2	47	423	11886			80%	5.1	1,180
Na	1471	33826	1164	26762	68	1552	0	11	239	5502			84%	4.8	21.6
B	743	8027	697	7532	19	201	0	1	27	294			96%	16.2	39.8
Li	749	5197	600	4163	14	100	0	2	134	932			82%	5.0	51.0
Al	530	14313	437	11785	0	0	0	13	93	2515			82%	5.7	1,100
Fe	264	14745	226	12640	0	5	0	16	37	2084			86%	7.0	700
Ca	231	9264	194	7793	0	13	1	43	35	1415			85%	6.3	166
K	194	7589	137	5356	26	1001	1	22	31	1210			84%	3.4	7.4
S	44	1419	24	757	5	154	0	1	16	507	12	397	92%	2.1	9.2
Mg	23	552	17	421	0	3	0	1	5	128			77%	4.2	178
P	12	380	10	305	0	0	0	4	2	70			82%	5.1	78.3
Cr	3	165	2	128	0	4	0	2	1	31			81%	4.5	29.5
Ni	1	74	1	87	0	1	0	1	0	(15)			121%		34.3
Cs	1	139	0	45	0	28	0	0	0	66			53%	1.5	4.9
Zn	1	52	1	47	0	1	0	3	0	1			98%	11.9	15.1
Cu	1	37	1	45	0	1	0	1	0	(10)			129%		16.3
Sr	0	14	0	16	0	0	0	0	0	(2)			115%		46.4
Mo	0	15	5	515	0	33	0	1	(6)	(533)			3615%		0.5
Gd	0	23	0	21	0	0	0	0	0	2			91%	11.0	566
Ru	0	10	0	5	0	0	0	0	0	5			56%	2.0	18.3
Ce	0	10	0	7	0	0	0	0	0	3			70%	3.3	231
Cl	27	944	26	930	9	302	0	0	(8)	(288)			131%	66.2	3.1
F	5	100	16	302	1	24	0	1	(12)	(226)			325%		4.1
NO3	1891	117234			19	1167	0	0	1872	116066	1,134	70,340	61%		
Total (no nitrate)		**157,362**		**128,192**		**3,427**		**169**		**25,573**		**397**	**84%**		

Table 6.3. Isokinetic samples material balance and closure value for each measured element.

	Feed	Glass	Offgas	Mass Balance	DF	
	moles	moles	moles	Closure	Glass	Offgas
Na	76.7	69.0	3.4	94%	10	23
B	51.6	38.1	2.2	78%	3.8	24
Li	40.5	36.0	< 1.2	92%	9.0	> 34
Al	28.7	23.8	< 0.0	83%	5.8	> 4300
Fe	14.7	12.2	0.0	83%	6.0	2100
Ca	12.5	10.5	< 0.1	84%	6.2	> 180
K	10.6	6.9	0.7	72%	2.9	16
Mg	1.22	0.77	0.00	63%	2.7	315
P	0.64	0.53	0.01	84%	5.7	81
Cr	0.15	0.14	< 0.01	94%	9.5	> 24
Ni	0.063	0.086	0.001	139%		59
Cs	0.057	0.029	< 0.033	109%	2.0	> 1.7
Zn	0.043	0.040	0.000	95%	18.0	86
Cu	0.031	0.043	< 0.001	143%		> 23
Sr	0.009	0.011	< 0.000	130%		> 75
Gd	0.008	0.007	< 0.000	91%	9.7	> 110
Mo	0.008	0.332	< 0.019	4641%		> 0.4
Ru	0.006	0.005	< 0.001	105%	25	> 11
Ce	0.004	0.003	< 0.000	72%	3.3	> 33

To clarify, Table 6.2 contains the data for the entire steady-state portion of the demonstration (i.e. glass was poured equivalent to three melter volumes). Table 6.3 contains the data *only* from the duration of the manual offgas samples, or approximately 3 hours of the steady-state portion of the test (the entire steady-state portion of the demonstration lasted almost 2 days).

While the fate of certain species are dealt with in section 6.5, the majority of the elements are well accounted for. There are some notable exceptions. Molybdenum clearly has a statistically significant deviation from 100%. This is most likely due to two facts: 1. The amount of molybdenum in the overall feed was quite small (~ 30 grams) and 2. The molybdenum electrodes and drain orifice experience erosion due to oxidation during the test. Based on the material balance, this erosion accounted for more than 1 kilogram of Molybdenum in the glass. This issue will be addressed in the second melter run by the replacement of the molybdenum drain and electrodes with Inconel 690.

6.4 Fate of Particular Species

Although the material balance for all elements is of interest towards the design and construction of the production vitrification facility, certain elements in SBW feed have a particular impact on the process. Understanding the fate of sulfur, nitrogen, water, surrogates for radioactive species, and halides will have influence on the number of unit operations, their sizing, and operation.

6.4.1 Fate of Sulfur

Because SBW feed is higher in sulfate than most melter feeds in the DOE complex, the fate of sulfur has the potential to drive the waste loading of the SBW glass. Table 6.4 shows the elemental percentages of sulfur in the glass versus the analyzed feed target percentage.

Table 6.4. Percentage of elemental sulfur in glass samples versus analyzed feed targets.

As-batched target wt% in glass	New target wt% in glass	Glass-106		Glass-147		Glass-161		Steady-State	
grams	wt%	wt%	% of Sulfur in Feed	wt%	% of Sulfur in Feed	wt%	% of Sulfur in Feed	wt%	% of Sulfur in Feed
0.40%	0.54%	0.15%	28%	0.25%	46%	0.29%	54%	0.31%	58%

This table shows the progression of the sulfur content in the glass over time. Glas-106 was the first glass sample taken. Glas-147 was taken after one melter turnover. Glas-161 was taken after two melter turnovers. The steady-state results are an average of the analyzed samples taken during steady state operating conditions (6 samples).

These results differ from those reported by Darab et al. (2001) (77% of sulfur in glass) as only a portion of steady-state glasses were considered there and they were compared to targeted sulfur concentrations in the feed. The end result is that 58% of the sulfur in the high-sulfur feed is retained in the glass. These results correspond well on a percentage basis with RSM-01-1 test glass that showed approximately 55% to 60% of the sulfur was retained in the glass (Goles et al. 2001). Roughly 28% of the sulfur was found in the offgas as SO_2, approximately 10% of the sulfur was captured in the scrub solution, and the remaining sulfur is unaccounted for.

It cannot be determined exactly at this point whether molten sulfate salt would have built up if the sulfate concentration were on target. Clearly there was more than enough elemental sulfur, given the results in section 5.6 and those in Table 6.7, to account for the molten salt mined from the melter surface after the demonstration. It is also clear that the glass retained as much if not more sulfate than the same formulation run in RSM-01-1. However, since some salt did appear in that RSM demonstration, one cannot conclude that no salt would have appeared in the EV-16 demonstration, although the results point in that direction. Regardless, a new formulation will be vitrified in the September demonstration, with hope that a minimal to non-existent sulfate salt layer will be evident.

6.4.2 Fate of Nitrogen

The material balance information for nitrogen and nitrate components is difficult to interpret. The first difficulty arises upon examination of the amount of nitrate (as determined by analysis of the feed samples) in the feed. The nitrate calculated from the batch sheet used to prepare the feed exceeds the feed nitrate analysis by almost 50%. This value either suggests interference in the analytical method (Ion Chromatography), resulting in poor recovery and low reported nitrate molarity or indicates that a lower amount of nitrate existed in the feed fed to the melter. The material balance does not support the later conclusion. The stream containing most of the nitrogen species is the offgas. The material balance for as-batched nitrate between the feed and the offgas indicates approximately 60% closure. . If the feed actually contained the amount of nitrate given by IC, this balance closure value would be closer to 120%, eliminating any possibility of reaction to Nitrogen. Furthermore, the major species in the waste simulant (Na, Al, K, Ca, Fe) were all added to the simulant as nitrate salts. Converting the ICP results for these components to the equivalent masses of nitrate added to the simulant agrees with the near 5 molar concentration expected.

6.4.3 Water Balance

The water balance shows that a good deal of water (approximately 420 kgs) was produced in the process. The obvious input sources of water to the melter were the slurry feed (approximately 50% liquid water), with an additional 97 g/L of waters of hydration from the hydrated salts. Additional water entered

through the humid South Carolina air, and this value was measured and accounted for. Based on the as-batched acidity of the feed, no more than 30 kgs of water could have resulted from titration of acid by the hydroxides in the glass formers.

6.4.4 Fate of Cesium

The levels of Cs retained in the glass often bordered on the lower detection limit of the AA system. Likewise, the Cs in the solids filtered from the feed samples was not detectable in any sample. Cs in the isokinetic offgas samples was not detected. The Cs in the scrub and filtered solids was detectable. Most if not all of the Cs that carried over into the offgas should have entered the scrub system. Given that, only 11.7% of the Cs was found in the scrub. This corresponds to a melter DF of 8.5, which is consistent with assumptions made in the design basis which, in turn, is based on data gathered at SRS and WVDP.

The uncertainty of this value is great. By the material balance calculations, only 44% of the Cs that was fed to the melter was detected in any of the output streams. It is recommended that this DF of 8.5 be applied with caution. If the 56% of the Cs that was not found ends up in the offgas system, this would lower to the melter DF for Cs to 1.47.

6.4.5 Fate of Halides

The test data are not very useful in determining the fate of the halides in the melter feed. Chloride and fluoride were detected in the feed, glass, and scrub solutions. Unfortunately, their material balance closure factors do not approach 100%. Fluoride in the feed often registered less than half of the batch calculated value, while Chloride was as often double that expected. Similar differences continue into the glass compositions. In all, these differences lead to the poor material balance closure values listed in Tables 6.1 and 6.2.

7. ENERGY BALANCE

7.1 Summary Energy Balance

Energy was supplied to the melter through electric power and through exothermic chemical reactions within the melter. Joule heating was the energy source in three “zones” within the melt. These were the two pairs of electrodes and the glass drain. A fourth “zone” of energy was transmitted via electrical resistance Kanthal heaters mounted in the melter lid. The lid temperature was kept within 600 ^{o}C – 800 ^{o}C to facilitate chemical reduction of nitrates enhance the melting rate.

Energy in the melter was used to evaporate water, heat and melt both glass components and the gaseous species within the melter. A relatively small amount of heat exited the melter with the product glass. A significant energy demand was the water flow through the cooling jacket surrounding the melter.

An energy balance around the EV-16 melter is shown in Table 7.1

Table 7.1. Summary energy balance.

Source	**Energy Input, KWH**
Electric Power	9,281
Net Chemical Reactions	416
Total	**9,697**
Demand	***Energy Utilization, KWH***
Evaporation of Water	940
Heating Gases in Plenum	2,603
Melter Jacket Cooling Water	6,218
Removal of Molten Glass	416
Total	**10,176**

7.2 Bases of Calculations

7.2.1 Electric Power Input

The DAS recorded power levels (in kw) in each of the four "zones" at ten-minute intervals. Zone 1 supplied power one pair of electrodes. Zone 2 powered the second pair of electodes. Zone 3 measured power passing between the zone 2 electrodes and the melter drain. Zone 4 was the power supplied to the plenum heaters. Energy supplied was calculated by averaging the power levels for adjacent 10-minute intervals and converting to kwh delivered during that interval. The DAS data set described in detail in Appendix E, and the DAS data that support the energy balance calculations are found in Appendix F. The total energy input was 2.35 MWhr/mton/day. As shown in Table 7.1, if the cooling water were not present, the energy input could have been reduced by 62%, yielding an energy input of 0.95 MWhr/mton/day.

7.2.2 Net Chemical Reactions

The impact of chemical reactions on the energy balance is a rough estimate at best. Nitrate salts can decompose thermally in the melter. However, the addition of a reducing agent such as sugar increases the number of possible reactions. From the batch sheet used to prepare feed for the test, the amount of sugar included in the feed was insufficient to react with all nitrate salts. Therefore, some of the salts decomposed thermally. Since the specific reactions involved cannot be known exactly, the energy transfer from chemical reactions is based on the assumed reactions listed in Table 10.2. Heats of reaction were determined using the following relationship: (heats of formation of products) – (heats of formation of reactants) [19]. Exothermic reactions have a negative sign. Endothermic reactions have a positive sign.

Table 7.2. Energy from chemical reactions.

Reaction	Energy Released or Absorbed per Mole of Nitrate Salt, kcal/g-mole	Gram-moles of Nitrate Salt Reacted	Total Energy Released or Absorbed, KWH
$C_{12}H_{22}O_{11} + 8NaNO_3 \rightarrow 4N_2 + 4Na_2O + 11H_2O + 8CO_2 + 4CO$	-82.8	1,903	-183.3
$2NaNO_3 \rightarrow 2NO_2 + Na_2O + 0.5O_2$	+60	2,527	+176.1
$2KNO_3 \rightarrow 2NO_2 + K_2O + 0.5O_2$	+82.7	422	+40.6
$C_{12}H_{22}O_{11} + 2Al(NO_3)_3 + 1.5\ O_2 \rightarrow 3N_2 + Al_2O_3 + 11H_2O + 6CO_2 + 6CO$	-397.6	1024	-473.2
$2Fe(NO_3)_3 \rightarrow 3NO_2 + Fe_2O_3$	+32.8	46.8	+1.8
$Ca(NO_3)_2 \rightarrow 2NO_2 + 0.5O_2$	+186.9	103.3	+22.4
Total			-415.7

7.3 Evaporation of Water

Based on an analysis of the feed material, a total of 1503 kgs (3306 lbs.) of water was calculated to be in the melter feed. The heat of vaporization used in the calculation was 970.3 BTU/lb [18].

7.4 Heating of Gases in Plenum

Off-gas measurements made by the off-gas monitoring contractor showed a steady-state off-gas flow rate of 57 scfm (at 68°F). The outside air to the film cooler was about 23 scfm. So the gas flow rate in the melter plenum was 34 scfm at 68°F. For the energy balance calculation, this flow was assumed to be constant for the entire test period. Including water added with the feed, water from decomposition of sugar, and water added from moist air inleakage, the total water content of the feed was approximately 12.1 scfm. Ignoring the COx and NOx content of the off-gas and assuming the remainder of the gas is air yields an overall composition of: 38.9% water vapor, 48.1% nitrogen, and 13% oxygen. An estimate for the heat capacity of this mixture was calculated from molal heat capacities for these gases to be 1.24 x 10^{-5} KHW/scf-^{o}C (Smith, 1959) The average increase in temperature of gas in the plenum was estimated at 585°C.

7.5 Heating of Glass

The heat capacity of the glass leaving the melter was calculated to be 2.7 x 10^{-4} KWH/kg-^{o}C (Perry, 1963) The total amount of glass produced was about 558 kg. With an exit temperature of about 1150°C, the amount of heat lost from the melter by pouring molten glass was about 169 KWH.

7.6 Sources of Error

The amounts of some species added to the melter are not known exactly. For example, chemical analysis of the feed indicates that the feed contained less than 4,000 gram-moles of nitrate as NO^{-3}. However, the batch sheet used to prepare the feed shows significantly more nitrate. Because of such measurement discrepancies, other quantities used in these calculations, such as the amount of water fed to the system may be in error. Some assumptions used in these calculations may also cause inaccuracy. The

assumption that off-gas airflow was constant at the same rate measured during steady state operation is probably not correct. For these reasons the values shown in Table 7.1should be viewed as estimates. This energy balance is best used simply to identify the major energy sources and sinks in the melter system.

8. CONCLUSIONS AND RECOMMENDATIONS

The amount of information that was gathered during this demonstration, both regarding positive test outcomes and lessons, provide an initial data set suitable to support pre-conceptual design activities for the full scale WVF. Referring back to the major test objectives:

- Demonstrate vitrification at maximum waste loading, demonstrate that the maximum waste loaded glasses produced on a bench scale could be processed at a pilot scale level, and produce acceptable waste forms per the product performance requirements

- Gather data necessary to support material and energy balance calculations around the melter unit operation

- Demonstrate the process at a pilot scale, observing process characteristics related to melting rate and cold cap behavior, performance of materials of construction, feed batching and handling, melter system operation, and offgas system and overall integrated process characterization in order to support engineering design of the production facility,

8.1 Waste Loading

The results of the demonstration and subsequent analysis show that an acceptable glass could be produced with 30 mass % of the uncorrected WM-180 composition and 70 mass% of SBW-9 additives. The PCT results indicate that the glass exceeded the current standard for durability. Viscosity and liquidus measurements showed that the glass also function within the operating parameters for which it was designed. However, a molten salt accumulated during the test. As stated, this accumulation could be explained by the higher than desired concentration of the sulfur in the feed, but the presence of molten salt in the RSM-01-1 test prevents this exclusive conclusion. The conclusion here is that the amount by which this salt accumulation exceeded those seen in other demonstrations was directly caused by the excess amount of sulfur in the feed. There would still, most likely, have been some salt if the feed concentration were on target, but not as much as was observed during this demonstration. The short-term impacts of this phase were mitigated during the test by addition of a reductant to the melt surface.

8.2 Material Balance

The analytical data have been evaluated and show good closure relative to the material balance. As noted during test operation, a good deal of feed material and other particulate matter was entrained in the offgas flow and deposited or retained in the offgas system. The DFs derived for the melter from these data are thought to be very conservative relative to the design of an offgas system based on these data. It is expected that the mitigation steps that have been identified for the second EV-16 melter demonstration in September will validate this thought and show general higher melter DFs for the SBW species. The fate of key components, such as sulfate, water, carbon, nitrate and NOx, halides, as well as that of the metals was understood to the degree possible given the melter system conditions. Results from the analyses have already impacted a new glass formulation for WM-180. Lessons learned from the demonstration will also change the operational condition assumptions for the next melter demonstration, and design bases that will impact the production facility.

Process observations made at the time of testing, combined with results garnered since that time, have given insight into areas where additional testing and engineering will be required to increase system reliability in the full scale facility design. The accretion of material in the offgas piping may be strongly tied to the excessive carryover conditions, but that conclusion will have to be validated in the second EV-16 demonstration. Molten salt accumulation will likely be addressed through glass formulation, although the presence of some amount of salt is beneficial to the melter throughput. Additional investigation in this area may be required to assess salt detection methods and limiting conditions for operations in the presence of molten salt, (assuming there are no corrosion and/or steam excursion/safety issues). Other assumptions relative to pilot scale and full-scale operations were confirmed and can be carried forth to design with greater confidence. The fulfillment of these objectives, along with the others listed, provide a successful basis for continued testing in the program.

8.3 Support of the Design Basis

In addition to these stated objectives, additional data are expected to be produced by the pilot scale vitrification test program. The data gathered in this test can be used to resolve uncertainties and validate assumptions . The HLW Program at the INEEL is relying upon the Technical Baseline Database (TBDB) as the design basis for ongoing design development. The TBDB gathers all the data that supports the vitrification flowsheet and its associated material and energy balance. A search of the database yields the elements where pilot scale testing is required to verify and/or validate assumptions currently being applied to design via verification and validation. Table 8.1 lists these elements, whether this demonstration has provided verification or validation, a very brief summary of the data, and a reference to what section in the report these data are found.

Table 8.1. Correlation of test results with technical baseline database.

Design Basis Element	**Addressed in this demonstration/ report**	**Summary of support information**	**Section where more detail can be found**
Volatilities of radionuclides (excluding Cs, Tc-99, and I-129) in melter	No		
Disposition/handling of noble metals in melter	No		
Carryover of melter feed to offgas	Yes	Melter offgas exit placement is critical to minimizing feed carryover, to be validated in second CETL test	4.2.5
Expected off-normal operations	Yes	Offgas plugging/fouling, molten salt accumulation, erosion/corrosion, feed pump, glass pour control issues were all experienced during this demonstration	4.2
Waste loading in glass	Yes	30% waste loading (SBW-9) met all requirements but did produce a molten sodium sulfate salt layer (accumulation of salt layer was due to additional amounts of sulfur fed to melter above the formulated amount)	5., 6.4.1

Choice of melter pilot test facility	No		
Recycle of radioactive process streams to melter	No		
Effects of recycled scrub on melter and glass	No		
Pressure control air requirement	No		
Partition factors for feed species in melter	Yes	Partition factors found within uncertainty of material balances	6.1, 6.2
Corrosion of melter components	Yes	Short term data gained on both oxidation of Mo components (not in baseline), and lack of corrosion of AZS refractory based on measurements	4.2.2
Melter feeding rate basis	Yes	A low feed range of 0.265 to 0.375 L/min was observed during the test	4.1.2
Film cooler outlet temperature	Yes	The film cooler outlet of 350°C was a control parameter based on DWPF experience	4.1.3
Slagging/plugging control at melter outlet	No*		
Reductant selection and concentration in melter feed	Yes	Sugar was used at 160 g/L SBW (31 grams Sugar/mole nitrate), producing Fe^{2+}/Fe_{total} ratios ranging from 0.10 to 0.19	5.5
Control of foaming in melter	Yes	Foaming was limited, either by operating conditions, reductant addition, or the combination thereof	
Chemistry of nitrate decomposition in melter	Yes	Nitrogen species effluents support the extent of reactions as described in section	5.7, 7.2
Melter air rate	Yes		5.7
Processing pressure in melter	Yes		5.7
Pumping behavior of melter feed slurry	Yes	The slurry remained suspended by the recirculating feed system and flowed well through the feed nozzle	
Speciation and partitioning of sulfate in melter	Yes	Incomplete results relative to sulfur balance closure give indications of SO3, Na2SO4, SO2, and $SO4^{2-}$ partitioning	4.1.1
Speciation of Iodine in melter offgas	No	Higher levels of iodine were added to the system, but a lack of an analytical method prevented the identification of partitioning factors for iodine	
Decomposition of	Yes	As the primary source of carbon (other	5.7

sugar in the melter		than tramp components), offgas effluent results of CO and CO2 indicate the extents of reaction for the decomposition of sugar	

8.4 Recommendation for future work

8.4.1 Molten Salt Formation/Accumulation

Additional testing is required to address open issues and to validate assumptions that exist in the TBDB. One key assumption is the waste loading, which will have a direct impact on the sizing and performance requirements of all process unit operations. This objective has not been met fully. The tie between glass formulation, redox ratio and control, and salt formation must be studied in detail. Since the first demonstration, strides have been made in the area of glass formulation and understanding of sulfate partitioning. These results have led to a new glass formulation that should control the accumulation of the molten sodium sulfate salt. This formulation will be used in the upcoming EV-16 demonstration. Again, it should be noted that the SBW-9 formulation was observed in the RSM-01-1 test to inhibit salt accumulation, but the EV-16 demonstration was run at a higher sulfate content. It is reasonable to conclude that the SBW-9 formulation would have prevented salt accumulation had the right amount of sulfate been present in the feed.

There are indications that the form and quantity of reductant added to the feed can impact the formation and accumulation of salts. Strong conclusions have not yet been drawn in this area, and the upcoming EV-16 demonstration, as well as additional effort using the RSM at PNNL will contribute to the understanding of redox impact on salt. Also, feed rate may impact the formation of salts. All of these potential drivers; formulation, redox control, and feed rate; must be evaluated with to gain a full understanding of the interactions and impacts. .

Given that molten salts accumulation is dependent upon the total amount of feed that has been fed to a melter over time, long-term testing is crucial to the elimination of this uncertainty. The determination of exactly when and at what level the molten salt accumulation stops at a steady-state value for a given glass formulation and redox ratio is a critical parameter that must be understood. Testing to this point has not been long enough in duration to understand this relationship, nor to understand the long term impacts of the presence of molten salts, including corrosion.

Until these many uncertainties with respect to the formation and accumulation of molten salts, specifically sodium sulfate salts, are resolved, the flowsheet proceeds with great risk. The potential for unqualified glass production, unacceptable melter life, and other operational safety issues do exist until this issue is eliminated or mitigated. This is the main focus of the development effort in the near future.

8.4.2 Changes in Melter Setup to Increase Data Certainty

Additional changes in the melter setup, data gathering, and sample gathering system will be made in the second demonstration. These changes are intended to improve the accuracy in determining material balance information that will flow down to design basis. As stated in section 4, some equipment modifications are being made to the melter to support this objective. The offgas outlet is being moved to the top of the plenum to reduce the deposition observed in the first demonstration. This should improve the offgas system reliability, resulting in improved steady state operating conditions.

In addition, the modifications will yield a more accurate depiction of melter DFs and thus reduce the load on the offgas system as it is perceived based on the test data presented herein, with regard to cesium DF, the feed will be spiked with an increased Cs concentration to meet minimum retention conditions. A new film cooler is being built to minimize the agglomeration of material in the offgas ductwork between the melter and the quench. Greater effort will be taken to characterize all of the accretions in the melter offgas piping to quantify their mass and composition. Similar improvements will be made to managing and tracking scrub accumulation, as well as characterizing the scrub solutions that remain in other units, such as the quench or HEME. Additional pressure taps will be placed across the various unit operations to improve detection and analysis of upsets to the offgas system, and maximize its effectiveness. These applications of the lessons learned from the first demonstration will provide additional validation for design bases and result in significant cost savings in the production facility.

The goal of this development is clear, to provide a continuity of scale between laboratory and research scale melter work to the eventual production system. Understanding the abilities of the melter to accomplish the goals of the facility is paramount. It is the critical unit operation to the vitrification system. The data gathered in these tests forms the basis for understanding the requirements, the production schedule, and the eventual costs (both project and operating) of the WVF. This demonstration builds a solid foundation for continued risk-reducing and cost-reducing effort coming in the near future.

9. REFERENCES

1. DOE, 1995, Consent Order and Settlement Agreement Between DOE and the State of Idaho Regarding Spent Fuel and Nuclear Waste Issues, October 17, 1995

2. The INEEL Spent Nuclear Fuel and Environmental Restoration and Waste Management Programs Environmental Impact Statement, DOE\EIS-0203-F, April, 1995.

3. Peeler, D. K., J. D. Vienna, T. B. Edwards, J. V. Crum, I. A. Reamer, M. J. Schweiger, R. J. Workman, "Glass Formulation Development for INEEL Sodium Bearing Waste (FY-2001 WM-180)," WSRC-TR-2001-00295, Rev. 0, Westinghouse Savannah River Company, Aiken, SC. .

4. Taylor, D., C. Barnes, L. Lauerhass, "INEL SBW Vitrification Process," INEEL/EXT-01-01139, September, 2001

5. Musick, C. A., B. A. Scholes, R. D. Tillotson, D. M. Bennert, J. D. Vienna, J. V. Crum, D. K. Peeler, I. A. Reamer, D. F. Bickford, J. C. Marra, and N. L. Waldo. *Technical Status Report: Vitrification Technology Development Using INEEL Run 78 Pilot Plant Calcine*, INEEL/EXT-2000-00110, Idaho National Engineering and Environmental Laboratory, Idaho Falls, Idaho. 2000.

6. Bennert, David., "Vitrification Demonstration Run Plan-DRAFT RELEASE - Vitrification Demonstration of Sodium Bearing Waste Surrogate Using WM-180 Simulant - Test SBW PS-FY01-1", INEEL/INT-2001-1073, March, 2001.

7. Barnes C. M. . "Feed composition for the Sodium-Bearing Waste Treatment Process," INEEL/EXT-2000-01378, Revision 1, July 2001.

8. Christian, J. D., "Composition and Simulation of Tank WM-180 Sodium-Bearing Waste at the Idaho Nuclear Technology and Engineering Center," INEEL/EXT-2001-00600, May, 2001.

9. Jantzen, C. M., N. E. Bibler, D. C. Beam, C. L. Crawford, and M. A. Pickett. *Characterization of the Defense Waste Processing Facility (DWPF) Environmental Assessment (EA) Glass Standard Reference Material (U)*, WSRC-TR-92-346, Revision 1, Westinghouse Savannah River Company, Aiken, South Carolina. 1993.

10. Bennert, David and Robert Wilson, "Vitrification Demonstration Run Plan-DRAFT RELEASE - Vitrification Demonstration of Sodium Bearing Waste Surrogate Using WM-180 Simulant - Test SBW PS-FY01-1", INEEL/INT-2001-1074, March 2001.

11. Goles, R. W., J. M. Perez, B. D. MacIsaac, D. D. Siemer, J. A. McCray, "Test Summary Report INEEL Sodium-Bearing Waste Vitrification Demonstration RSM-01-1," PNNL-13522, May 2001. .

12. Kuhn, Bill, memo to Langdon Holton re: "Analysis of Potential for a Water/Molten Salt Vapor Explosion", April 1983.

13. R. H. Doremus, "Glass Science," John Wiley & Sons, New York, 1973. Standard Practice for Measuring Viscosity of Glass Above the Softening Point," ASTM C-965-95, 1995.

14. American Society for Testing and Materials, "Standard Test Method for Determining Chemical Durability of Nuclear Waste Glasses, The Product Consistency Test (PCT)," ASTM-C-1285-97, 1998

15. J. D. Vienna, D. K. Peeler, C. M. Jantzen, J. V. Crum and L. Bruckner, "Standard Test Methods for Determining the Liquidus Temperature (T_L) of Waste and Simulated Waste Glasses," Submitted to ASTM C26.13 for Committee Ballot, 1998 American Society for Testing and Materials.

16. D. K. Peeler, I. A. Reamer, J. D. Vienna and J. V. Crum, *Technical Status Report: Preliminary Glass Formulation Report for the INEEL HAW*, WSRC-TR-98-0012, Rev. 1, March, 1998. .

17. Weast, R.C., ed., Handbook of Chemistry and Physics, 56th ed., CRC Press, Cleveland, OH, 1975, pp. D-67

18. Perry, R. H. & Green, D. W. Perry's Chemical Engineers' Handbook, 4th ed., 1963. p.3-191

19. Smith, J. M. and H. C. Van Ness, Introduction to Chemical Engineering Thermodynamics, 2nd ed., McGraw-Hill, New York, 1959, p. 122.

20. McCray, J. A. and Griffith, D. L., "A Snapshot of Melt Rate Testing And Reductant Selection for the INEEL Sodium-Bearing Waste Vitrification Program," The American Ceramic Society 103rd Annual Meeting and Exposition, paper B4D-08-2001, April 2001

21. Wilson, R.A. "Vitrification of Mixed Waste Surrogate Sludges at Rocky Flats Plant", Master of Science Thesis – Clemson University, Environmental Systems Engineering. May 1996.

22. Fogler, H.S. "Elements of Chemical Reaction Engineering", Prentice-Hall, Inc., Englewood Cliffs, New Jersey. 1996.